Supporting Information

***Rec. Nat. Prod*. 18:5 (2024) 514-519**

Potent Cytotoxicity and Nitric Oxide Suppression of Compounds Derived from *Kaempferia elegans* Rhizomes: Molecular Modeling on EGFR Inhibition

Kongdech Savaspun[1,2], Chutamas Thepmalee [3], Hla Myo [4], Apiwan Arinno[5], Anuchit Phanumartwiwath[4], Chanat Aongbangkhen[5], Chatchakorn Eurtivong[6], Siriwat Boonchaisri[2,7], Padarat Ninjiaranai[8], Pornpat Sam-ang[8]*

[1]Division of Chemistry, School of Science, University of Phayao, Phayao 56000, Thailand
[2]Traditional Lanna Medicine Research Group, School of Science, University of Phayao, Phayao 56000, Thailand
[3]Division of Biochemistry, School of Medical Sciences, University of Phayao, Phayao 56000, Thailand
[4]College of Public Health Sciences, Chulalongkorn University, Bangkok 10330, Thailand
[5]Center of Excellence in Natural Products Chemistry (CENP), Department of Chemistry, Faculty of Science, Chulalongkorn University, Bangkok, 10330, Thailand
[6]Department of Pharmaceutical Chemistry, Faculty of Pharmacy, Mahidol University, Bangkok 10400, Thailand
[7]Division of Biology, School of Medical Sciences, University of Phayao, Phayao 56000, Thailand
[8]Division of Chemistry, Faculty of Science and Technology, Pibulsongkram Rajabhat University, Phitsanulok 65000, Thailand

Table of Contents	Page

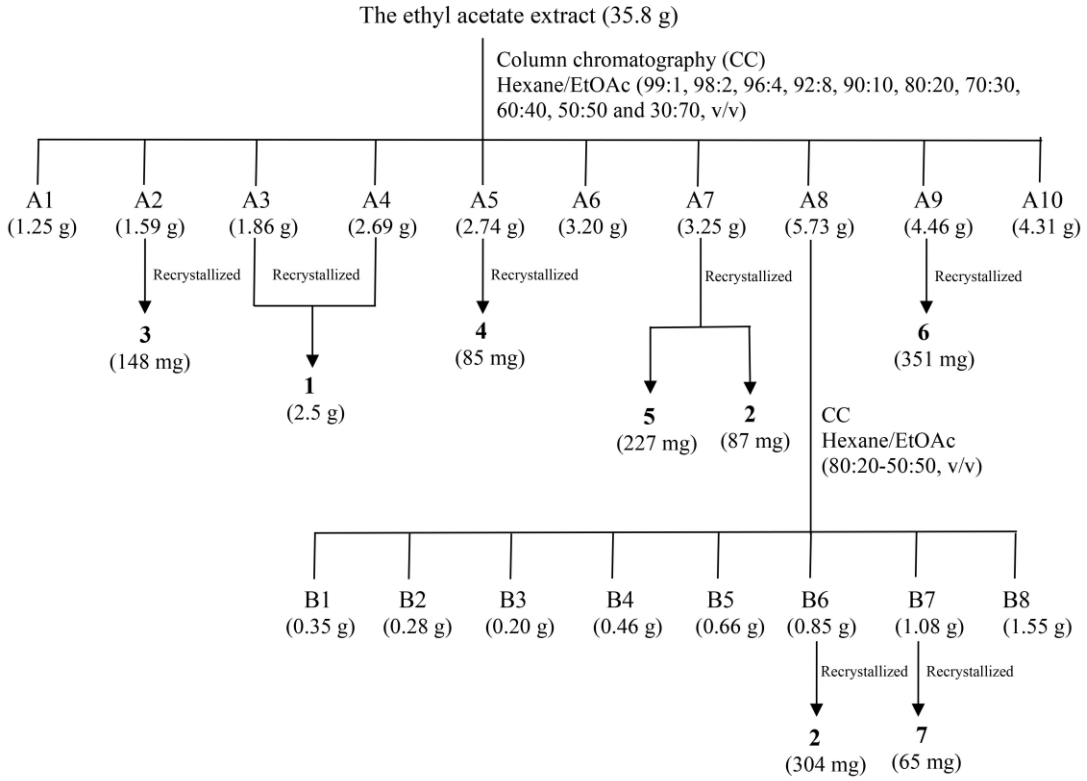

Scheme S1: Isolation of pure compounds **1**–**7**

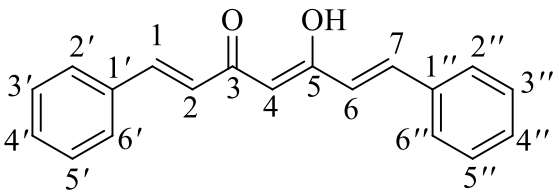

Table S1: ^{1}H NMR, ^{13}C NMR, COSY and HMBC data of **3** in $CDCl_3$

	3			
Position	δ_H	δ_C	COSY	HMBC
1, 7	7.66[a] (2H, *d*, *J* = 15.8)	140.6[a]	2, 6	C-2/C-6, C-2′/C-6′/C-2″/C-6″
2, 6	6.63[b] (2H, *d*, *J* = 15.8)	124.1[b]	1, 7	C-1′/C-1″
3	-	183.3[c]		
4	5.85 (1H, *s*)	101.8[d]		C-2/C-6
5	-	183.3[c]		
1′, 1″	-	135.0[e]		
2′, 2″	7.55[c] (2H, *br dd*, *J* = 7.8 and 2.2 Hz)	128.1[f]	3′, 3″	C-1/C-7, C-4′/C-4″/C-6′/C-6″
3′, 3″	7.39[d] (2H, *m*)	129.0[g]	2′, 2″	C-1′/C-1″/C-2′/C-2″
4′, 4″	7.39[d] (2H, *m*)	130.1[h]		C-2′/C-2″/C-6′/C-6″
5′, 5″	7.39[d] (2H, *m*)	129.0[g]	6′, 6″	C-1′/C-1″/C-3′/C-3″
6′, 6″	7.55[c] (2H, *br dd*, *J* = 7.8 and 2.2 Hz)	128.1[f]	5′, 5″	C-1/C-7, C-2′/C-2″/C-6′/C-6″
5-OH	15.91 (1H, *br s*)			

[a, b, c, d, e and f] Overlapping signals with the same superscript.

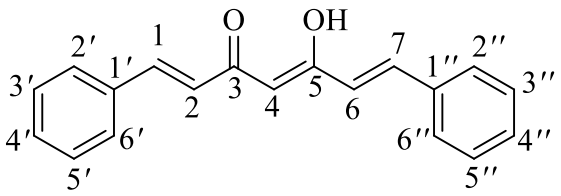

Table S2: NMR data of **3** and (1*E*,4*Z*,6*E*)-5-hydroxy-1,7- diphenylhepta-1,4,6-trien-3-one

No.	**3**		**(1*E*,4*Z*,6*E*)-5-Hydroxy-1,7-diphenylhepta-1,4,6-trien-3-one** [1]	
	δ_H, Mult. (*J* in Hz)[a]	δ_C[a]	δ_H, Mult. (*J* in Hz)[b]	δ_C[b]
1	7.66 (*d*, 15.8)	140.7	7.67 (*d*, 16.0)	140.3
2	6.63 (*d*, 15.8)	124.1	6.96 (*d*, 16.0)	124.3
3	-	183.3	-	183.2
4	5.85 (*s*)	101.8	6.21 (*s*)	101.7
5	-	183.3	-	183.2
6	6.63 (*d*, 15.8)	124.1	6.96 (*d*, 16.0)	124.3
7	7.66 (*d*, 15.8)	140.7	7.67 (*d*, 16.0)	140.3
1′	-	135.0	-	135.0
2′	7.55 (*br dd*, 7.8, 2.2)	128.4	6.93 (*dd*, 8.0, 2.0)	128.3
3′	7.39 (*m*)	129.0	7.45 (*m*)	129.0
4′	7.39 (*m*)	130.1	7.45 (*m*)	130.3
5′	7.39 (*m*)	129.0	7.45 (*m*)	129.0
6′	7.55 (*br dd*, 7.8, 2.2)	128.4	6.93 (*dd*, 8.0, 2.0)	128.3
1″	-	135.0	-	135.0
2″	7.55 (*br dd*, 7.8, 2.2)	128.4	6.93 (*dd*, 8.0, 2.0)	128.3
3″	7.39 (*m*)	129.0	7.45 (*m*)	129.0
4″	7.39 (*m*)	130.1	7.45 (*m*)	130.3
5″	7.39 (*m*)	129.0	7.45 (*m*)	129.0
6″	7.55 (*br dd*, 7.8, 2.2)	128.4	6.93 (*dd*, 8.0, 2.0)	128.3
5-OH	15.91 (*br s*)	-	-	-

Recorded in [a] $CDCl_3$ (400 MHz for ^1H NMR, 100 MHz for ^{13}C NMR), [b] DMSO-d_6 (500 MHz for ^1H NMR, 125 MHz for ^{13}C NMR)

[1] V.T.B. Pham, T.V. Nguyen, H.V. Nguyen, T.T. Nguyen, H.M. Hoang (2020). Curcuminoids versus pyrazole-modified analogues: synthesis and cytotoxicity against HepG2 cancer cell line, *ChemistrySelect* **5**, 11681.

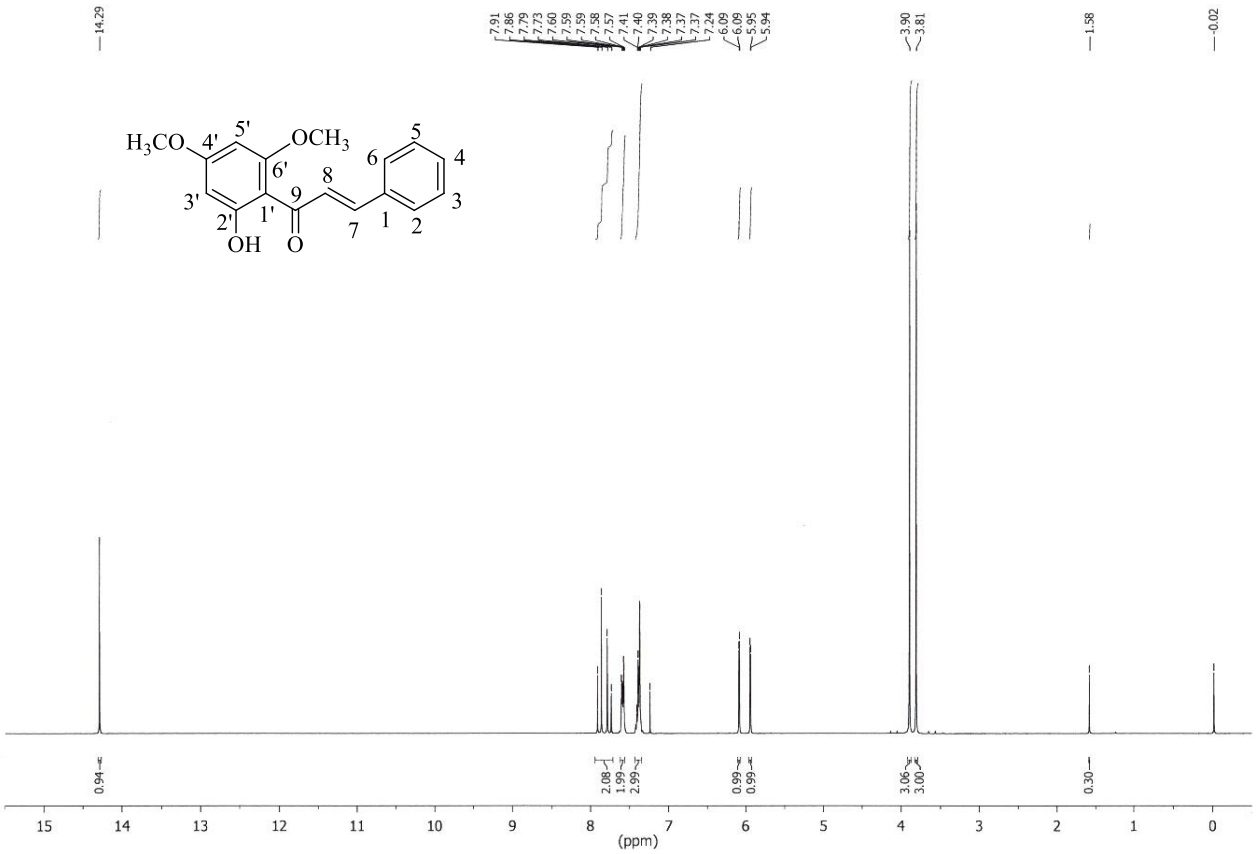

Figure S1: ^{1}H NMR spectrum of **1** (300 MHz, $CDCl_3$)

^{1}H NMR δ: 14.29 (*s*, 2′-OH, 1H), 7.89 (*d*, *J* = 15.0 Hz, H-7, 1H), 7.76 (*d*, *J* = 15.0 Hz, H-8, 1H), 7.59 (*m*, H-2, H-6, 2H), 7.39 (*m*, H-3, H-4, H-5, 3H), 6.09 (*d*, *J* = 2.4 Hz, H-3′, 1H), 5.94 (*d*, *J* = 2.4 Hz, H-5′, 1H), 3.90 (*s*, 6′-OCH_3, 3H), 3.81 (*s*, 4′-OCH_3, 3H)

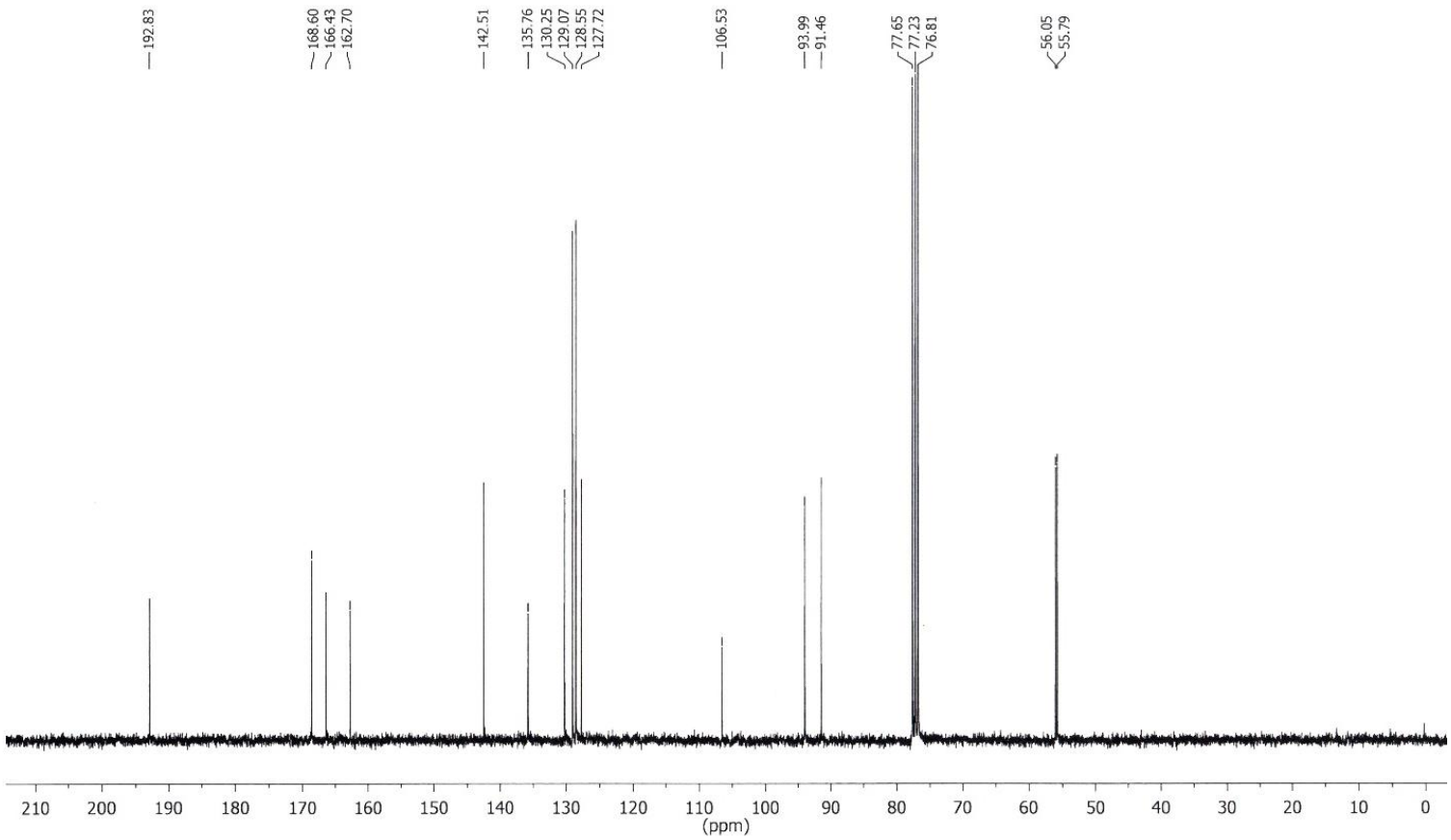

Figure S2: ^{13}C NMR spectrum of **1** (75 MHz, $CDCl_3$)

^{13}C NMR (75 MHz, $CDCl_3$, ppm) δ: 192.8, 168.6, 166.4, 162.7, 142.5, 135.8, 130.3, 129.1 (2C), 128.6 (2C), 127.7, 106.5, 94.0, 91.5, 56.1(2C), 55.8. mp. 93.5–94.5 ^{o}C

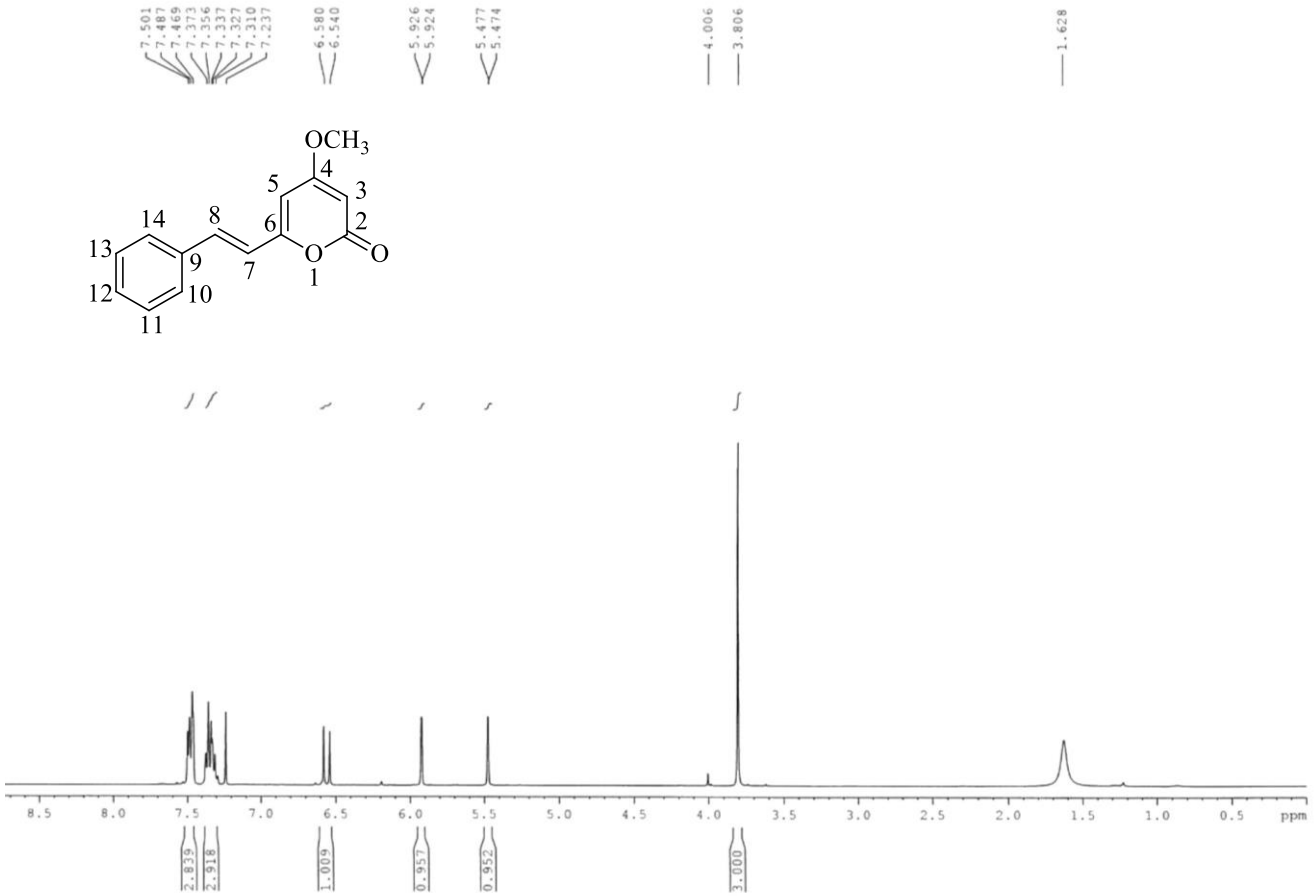

Figure S3: ^{1}H NMR spectrum of **2** (400 MHz, $CDCl_3$)

^{1}H NMR δ: 7.48 (2H, *m*, H-10 and H-14), 7.48 (1H, *d*, *J* = 16.0 Hz, H-8), 7.34 (3H, *m*, H-11, H-12 and H-13), 6.56 (1H, *d*, *J* = 16.0 Hz, H-7), 5.93 (1H, *d*, *J* = 0.8 Hz, H-5), 5.48 (1H, *d*, *J* = 0.8 Hz, H-3), 3.81 (3H, *s*, 4-OCH_3)

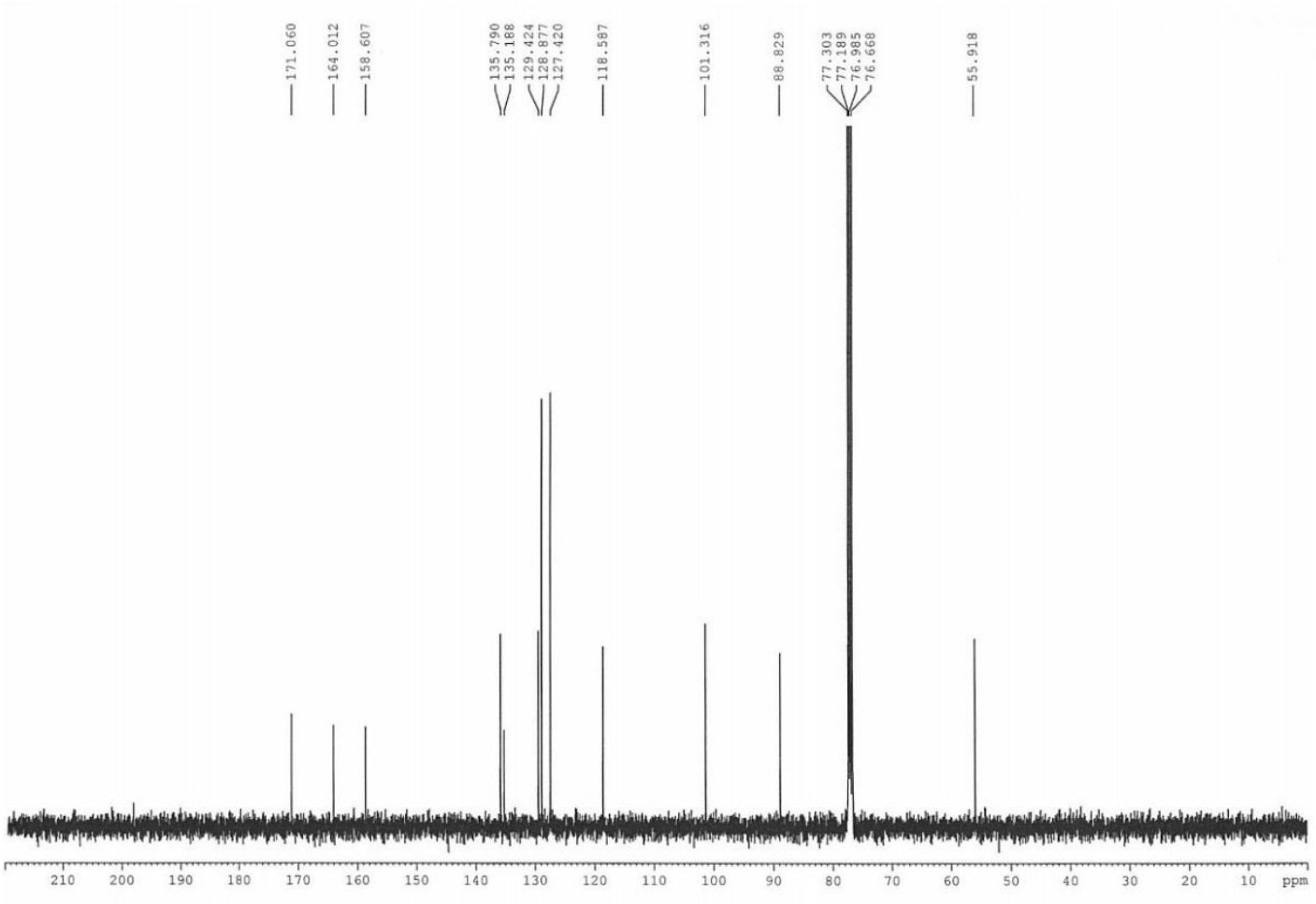

Figure S4: ^{13}C NMR spectrum of **2** (100 MHz, $CDCl_3$)

^{13}C NMR δ: 171.1, 164.0, 158.6, 135.8, 135.2, 129.4, 128.9 (2C), 127.4 (2C), 118.6, 101.3, 88.8, 55.9. mp. 140–141^{o}C

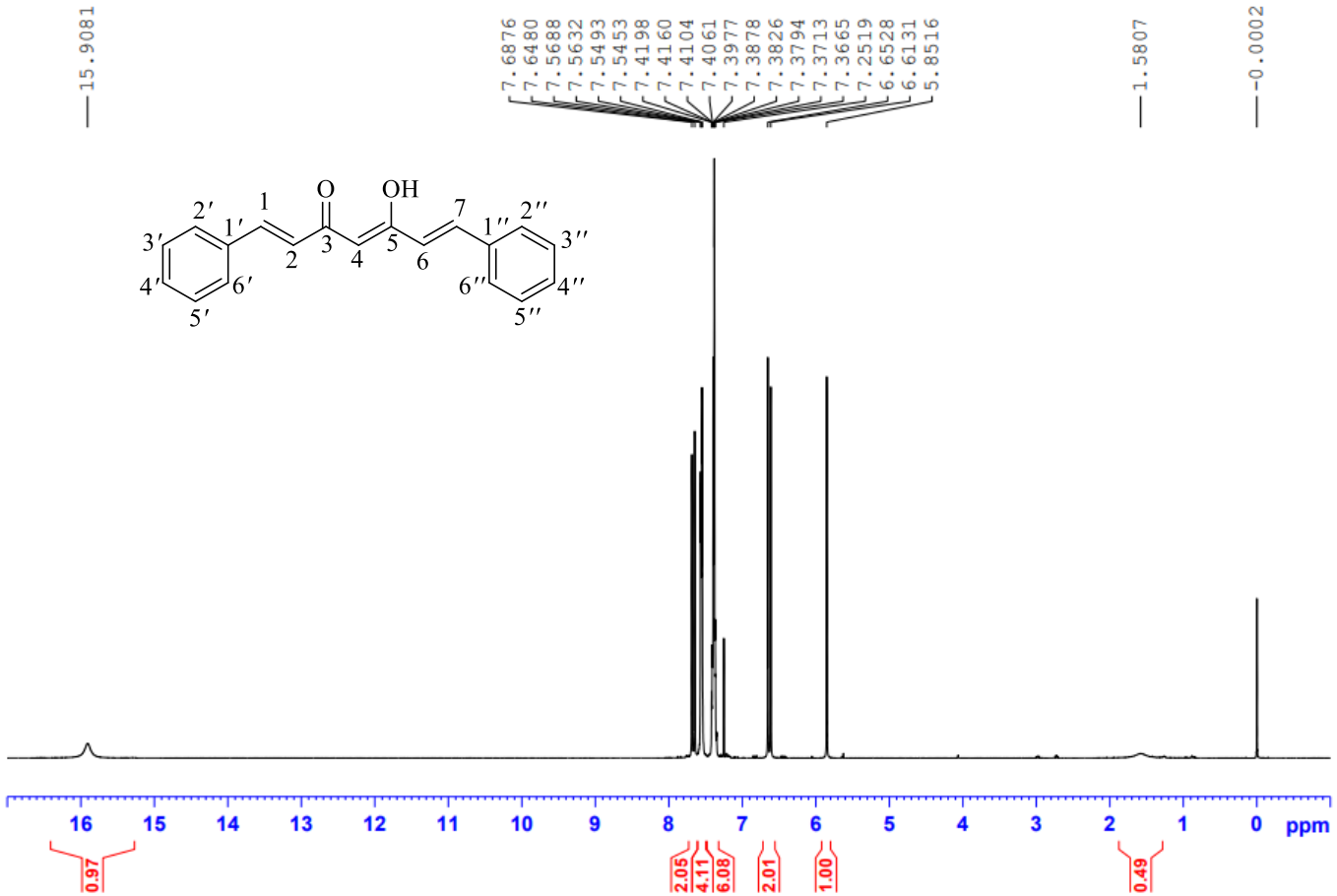

Figure S5: ^{1}H NMR spectrum of **3** (400 MHz, $CDCl_3$)

^{1}H NMR δ: 15.91 (*br s*, 5-OH, 1H), 7.66 (*d*, *J* = 15.8 Hz, H-1 and H-7, 2H), 7.55 (*br dd*, *J* = 7.8 and 2.2 Hz, Ar-H, 4H), 7.39 (*m*, Ar-H, 6H), 6.63 (*d*, *J* = 15.8 Hz, H-2 and H-6, 2H), 5.85 (*s*, H-4, 1H)

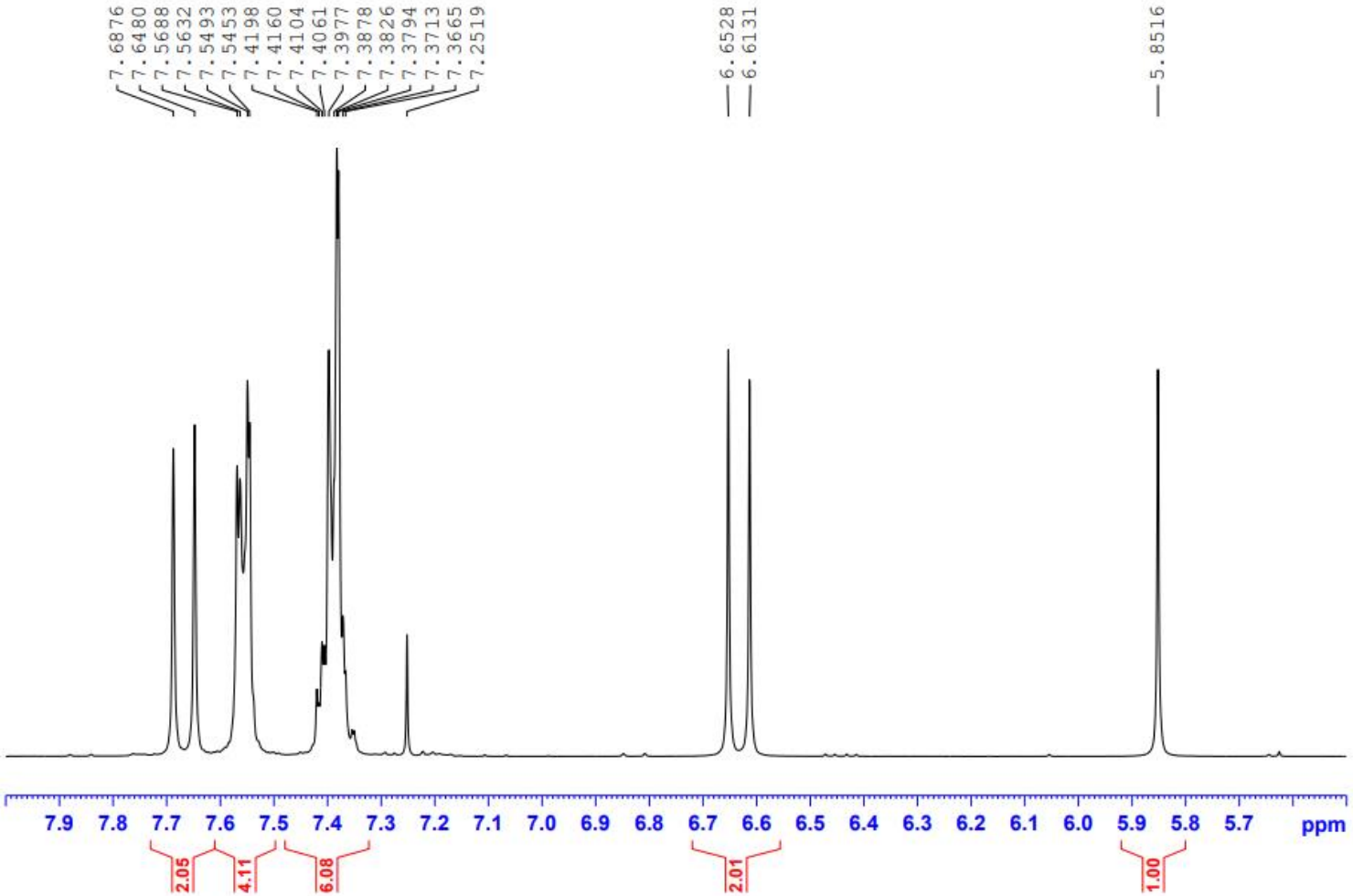

Figure S5.1: Expansion of ^{1}H NMR spectrum of **3** (400 MHz, $CDCl_3$)

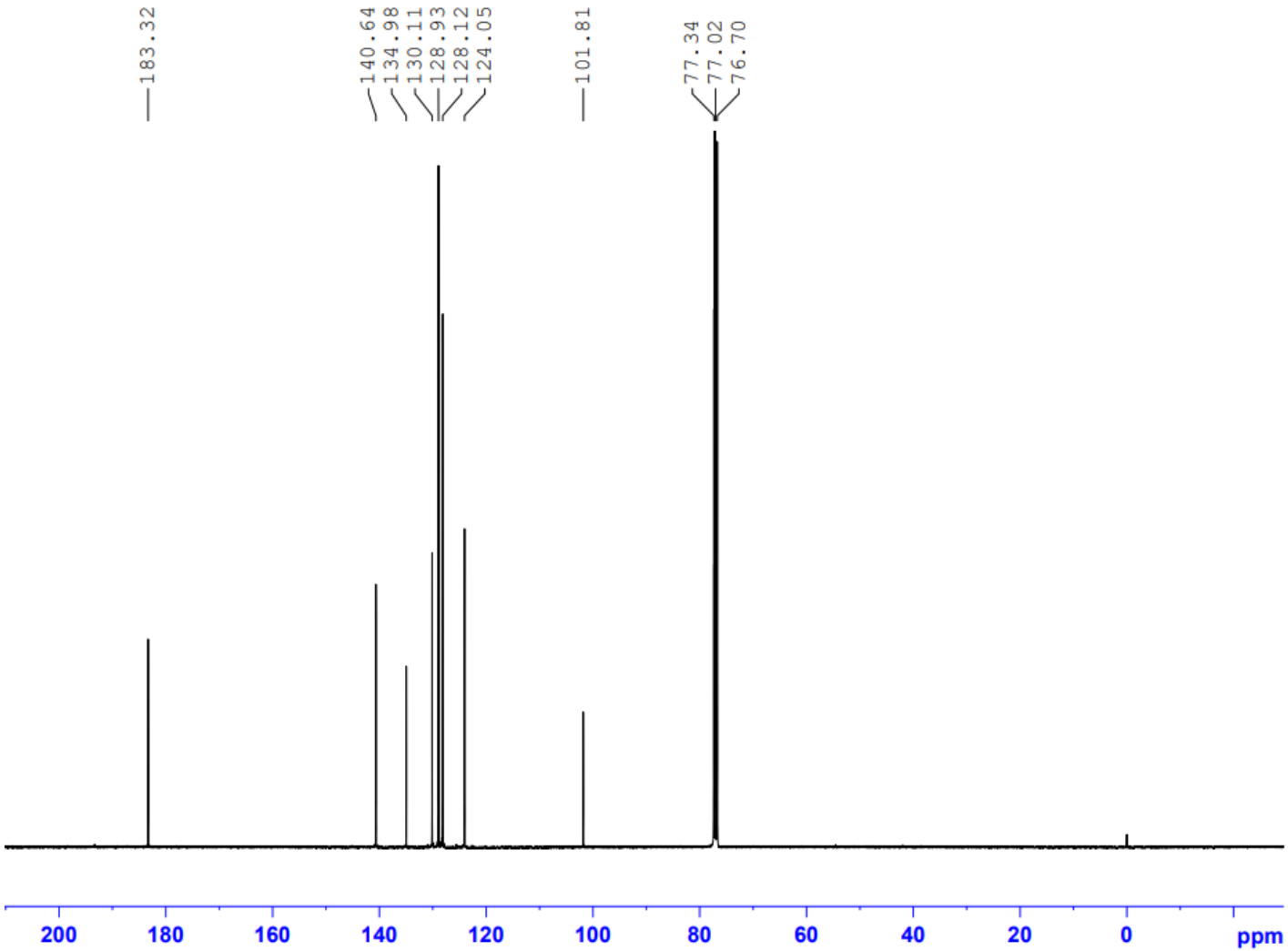

Figure S6: ^{13}C NMR spectrum of **3** (100 MHz, $CDCl_3$)

^{13}C NMR δ: 183.3, 140.6, 135.0, 130.1, 129.0, 128.1, 124.1, 101.8. mp. 140.2–142.0 ^{o}C

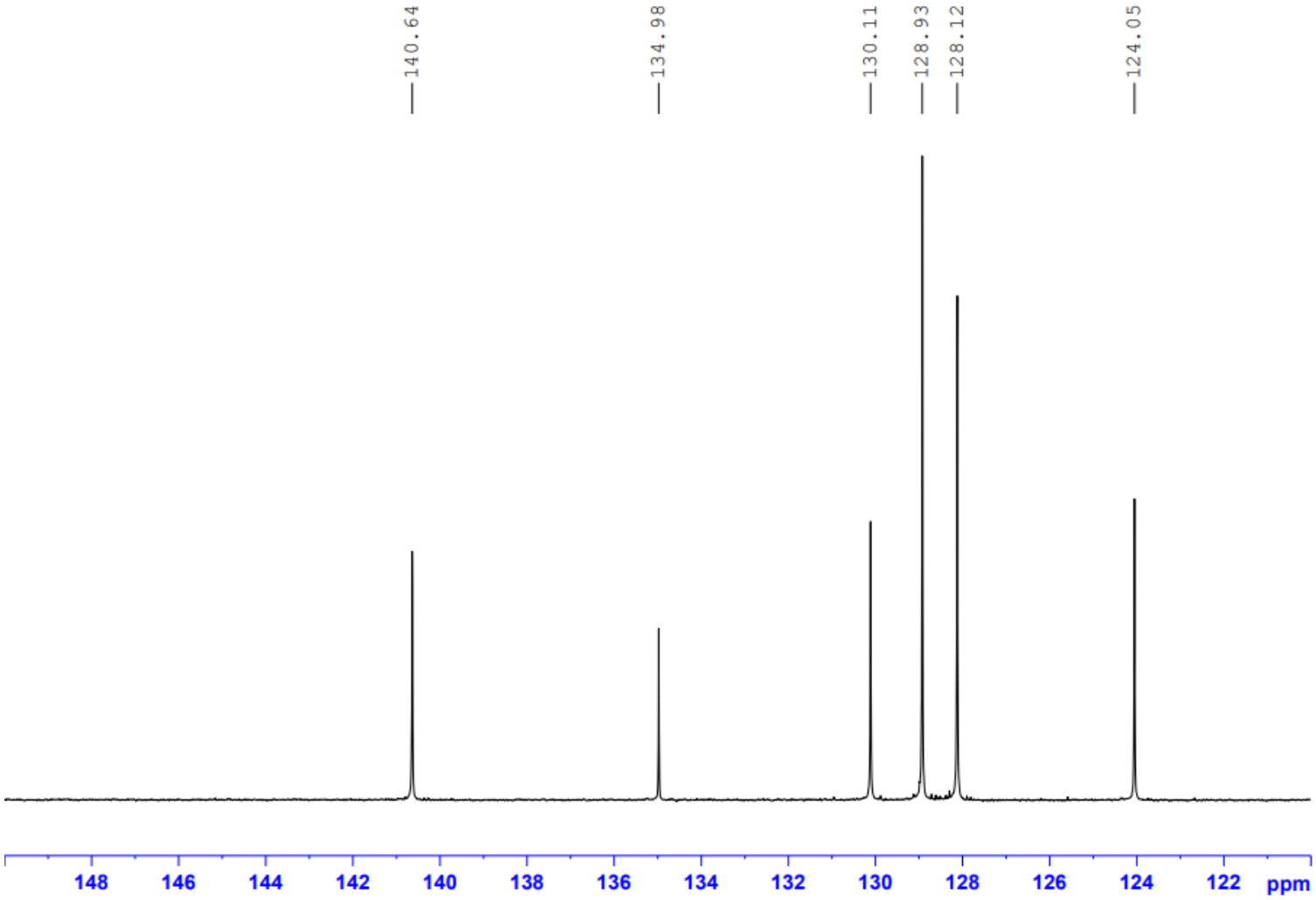

Figure S6.1: Expansion of ^{13}C NMR spectrum of **3** (100 MHz, $CDCl_3$)

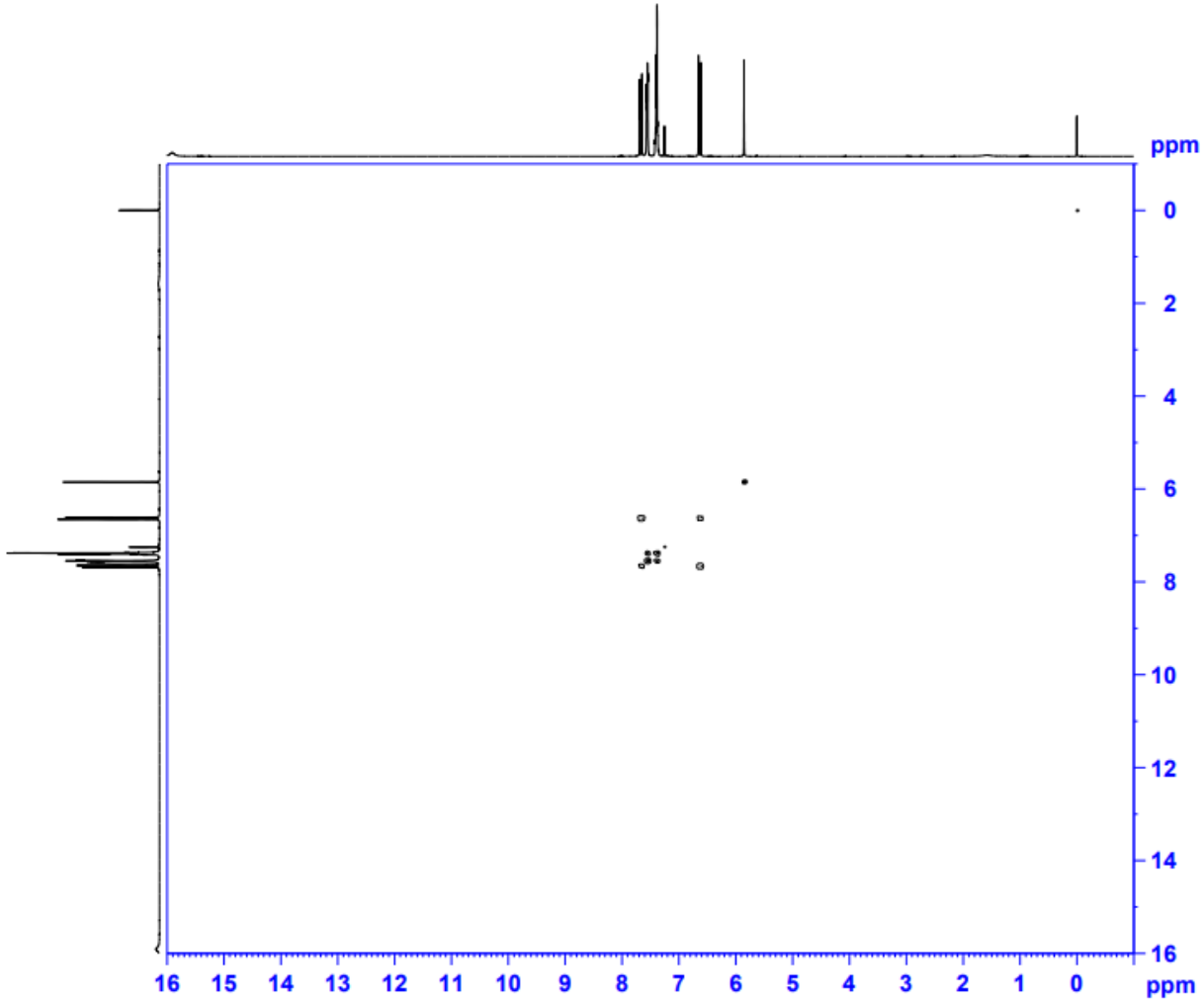

Figure S7: COSY spectrum of **3** ($CDCl_3$)

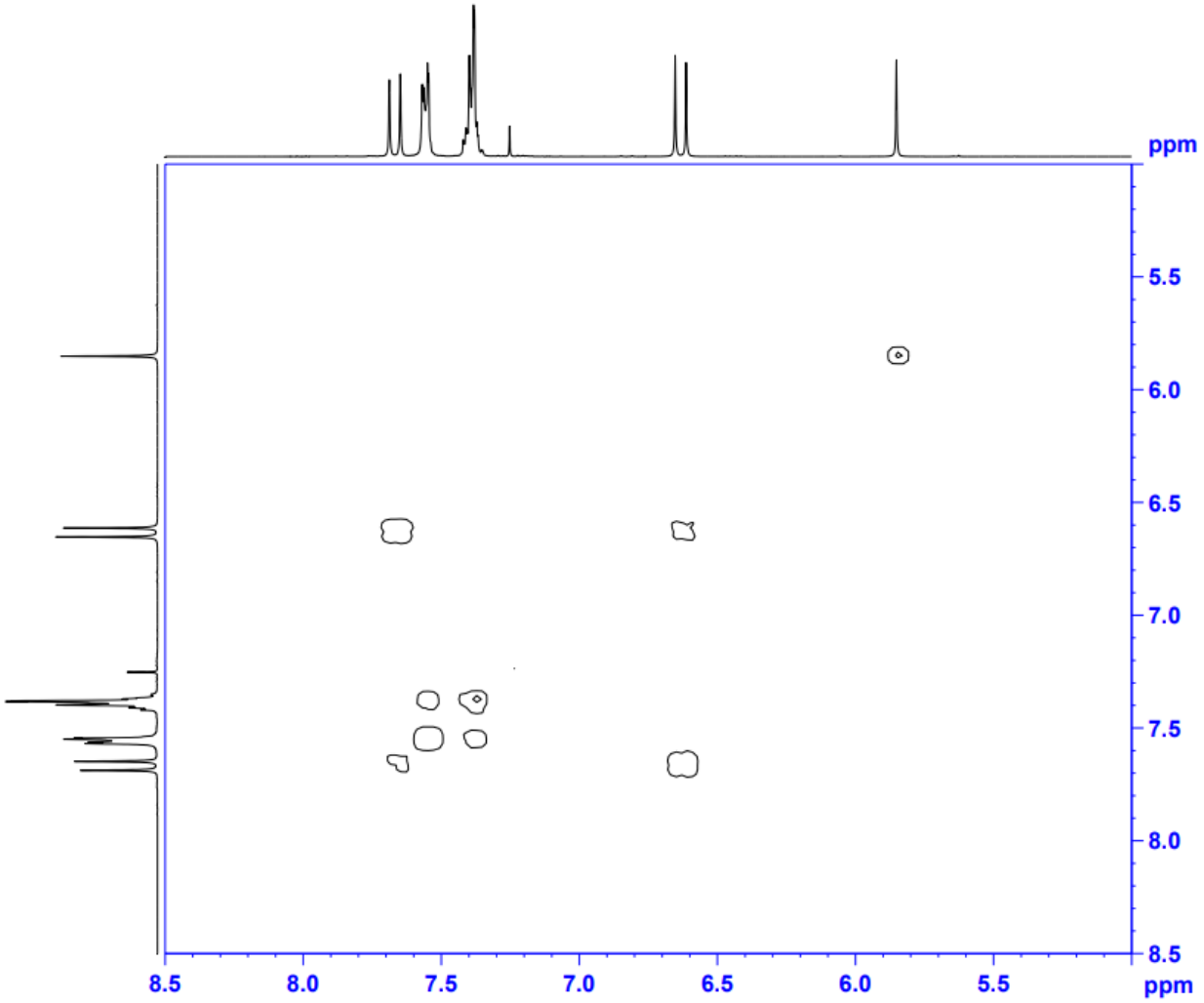

Figure S7.1: Expansion of COSY spectrum of **3** ($CDCl_3$)

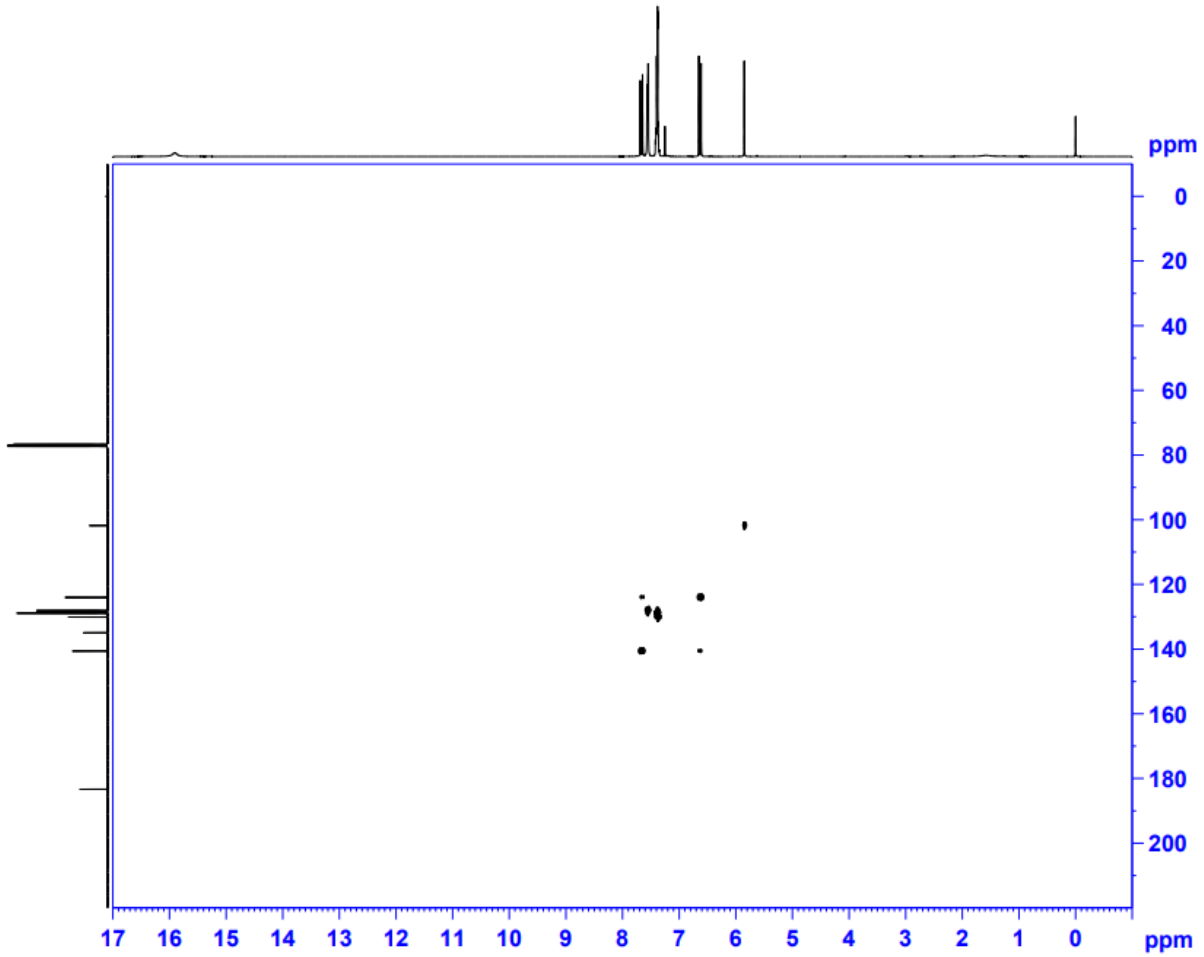

Figure S8: HSQC spectrum of **3** ($CDCl_3$)

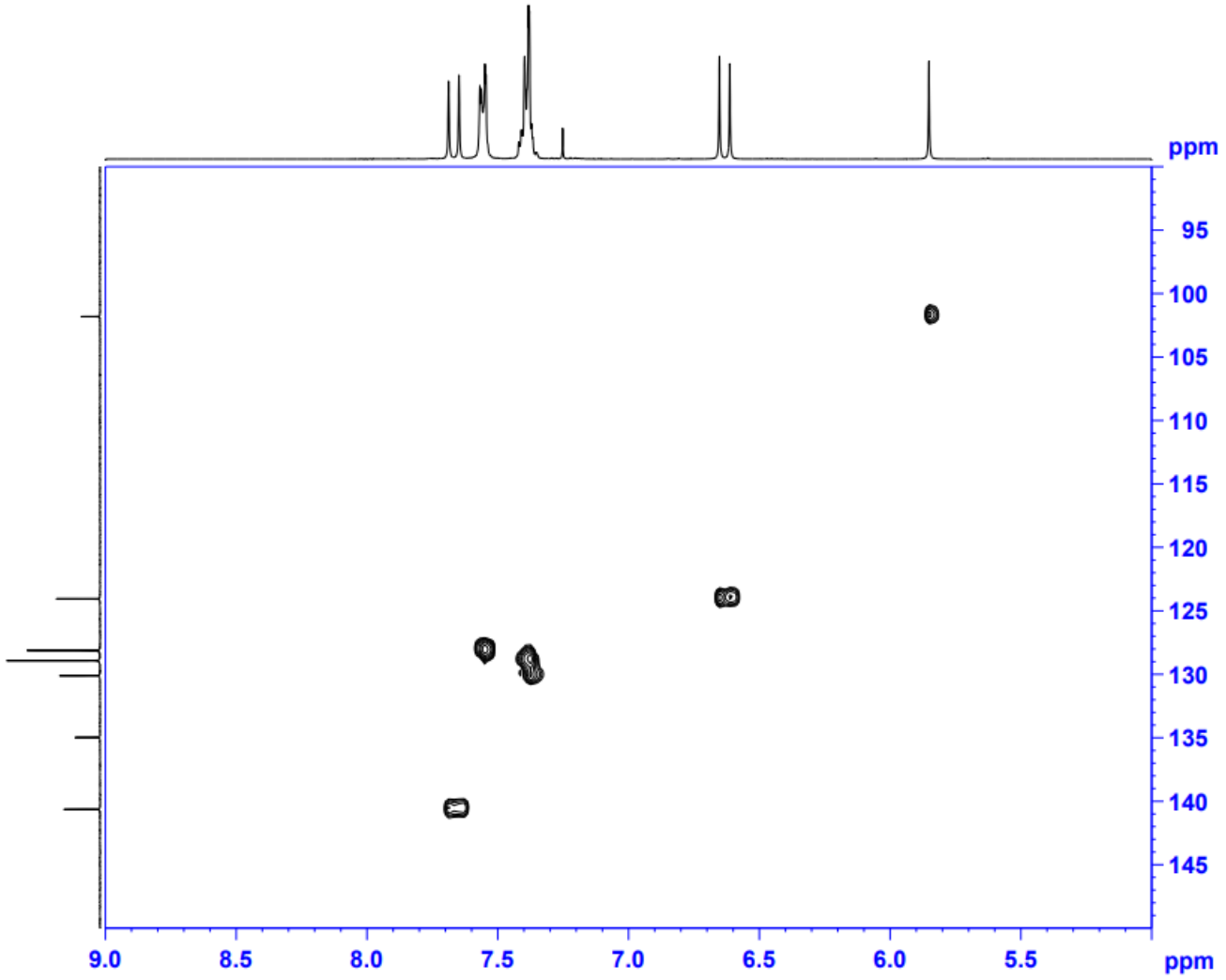

Figure S8.1: Expansion of HSQC spectrum of **3** ($CDCl_3$)

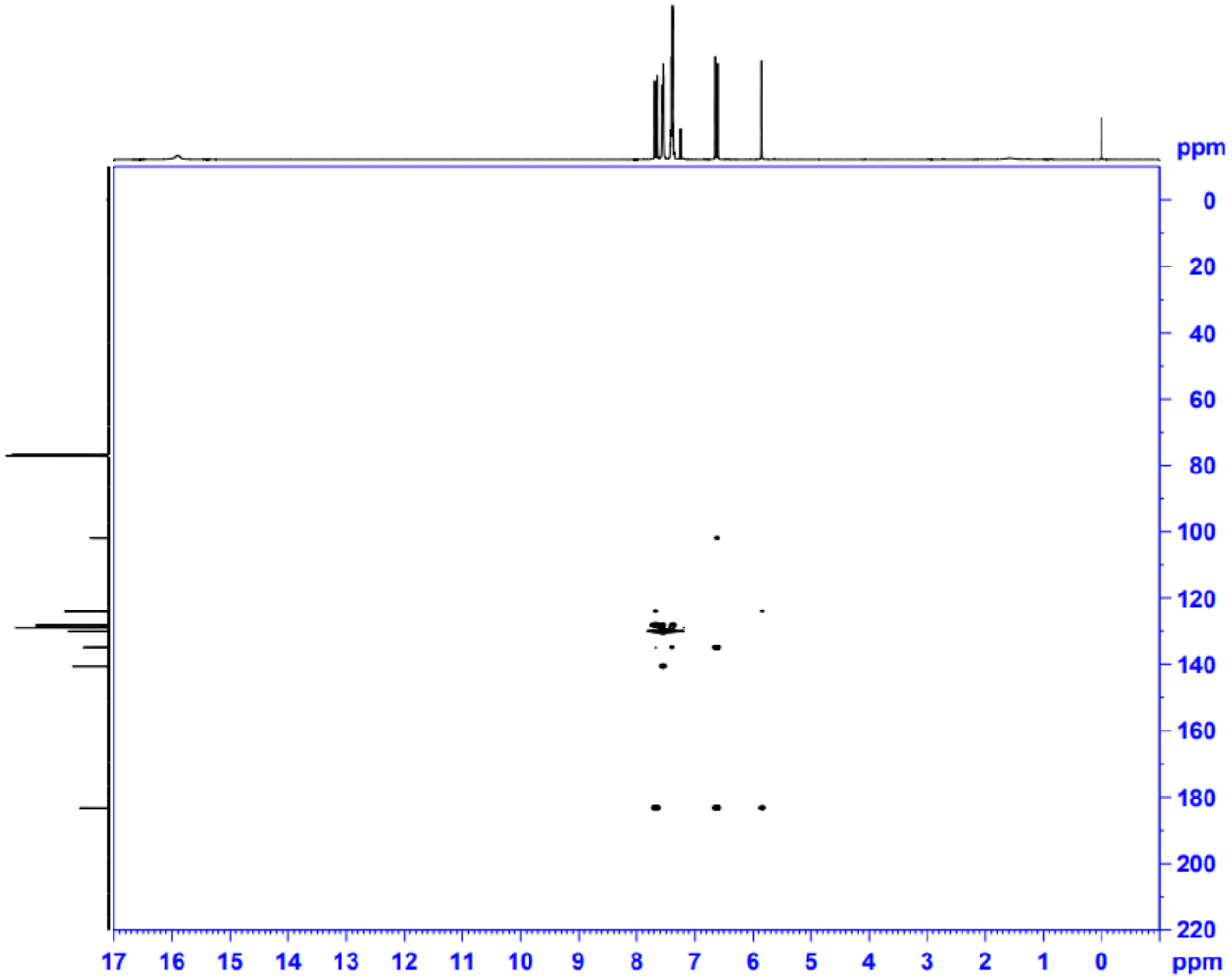

Figure S9: HMBC spectrum of **3** ($CDCl_3$)

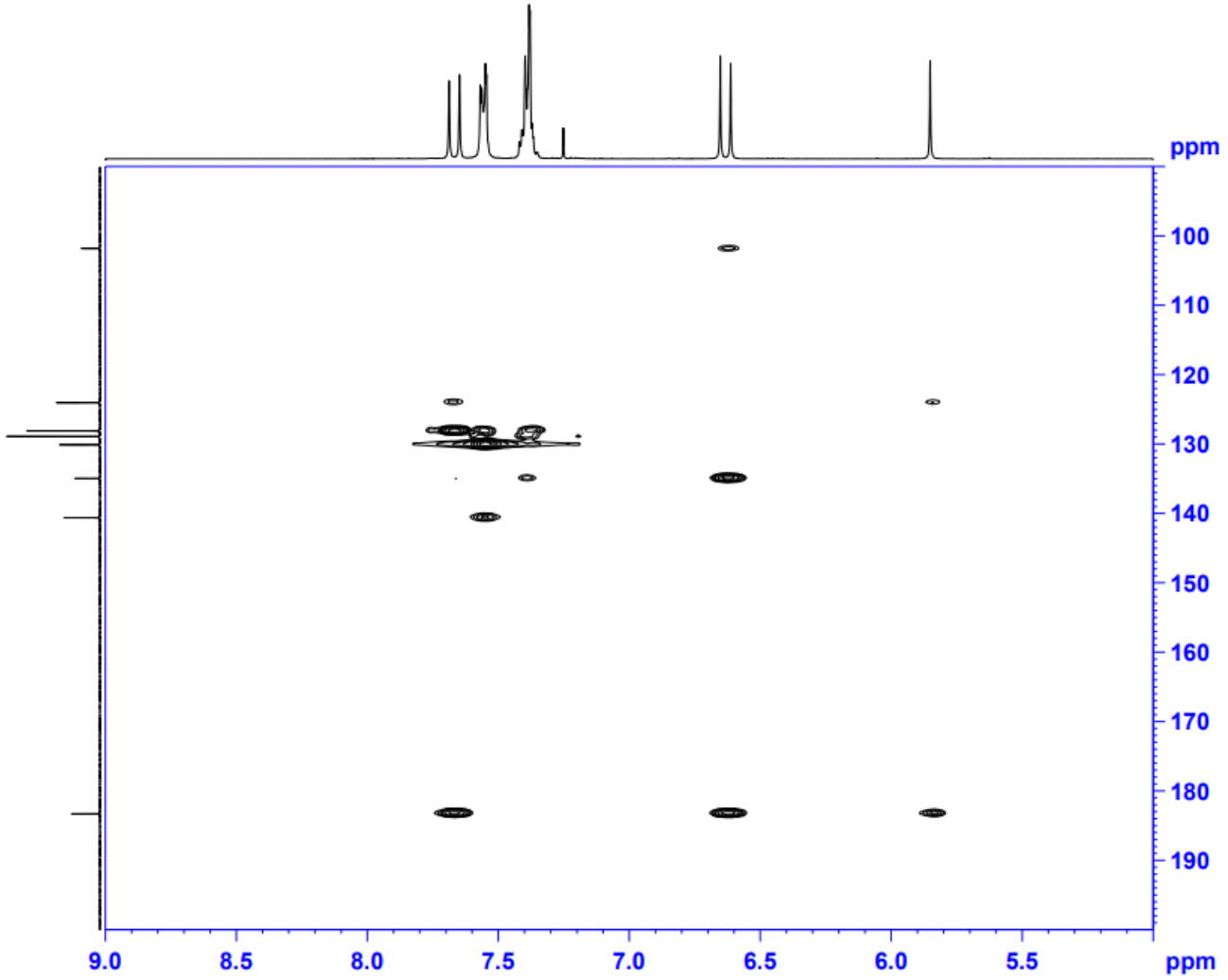

Figure S9.1: Expansion of HMBC spectrum of **3** ($CDCl_3$)

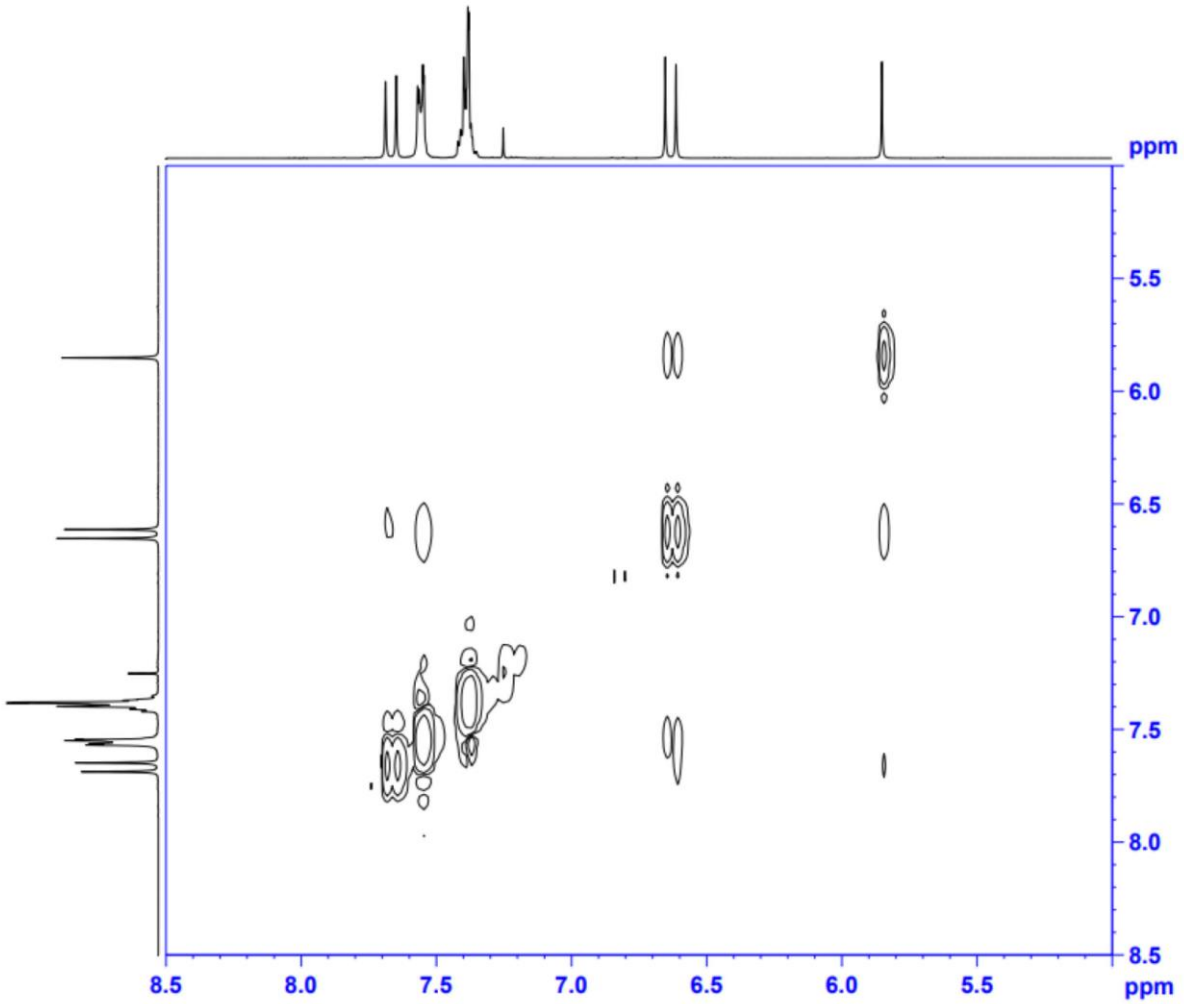

Figure S10: NOESY spectrum of **3** ($CDCl_3$)

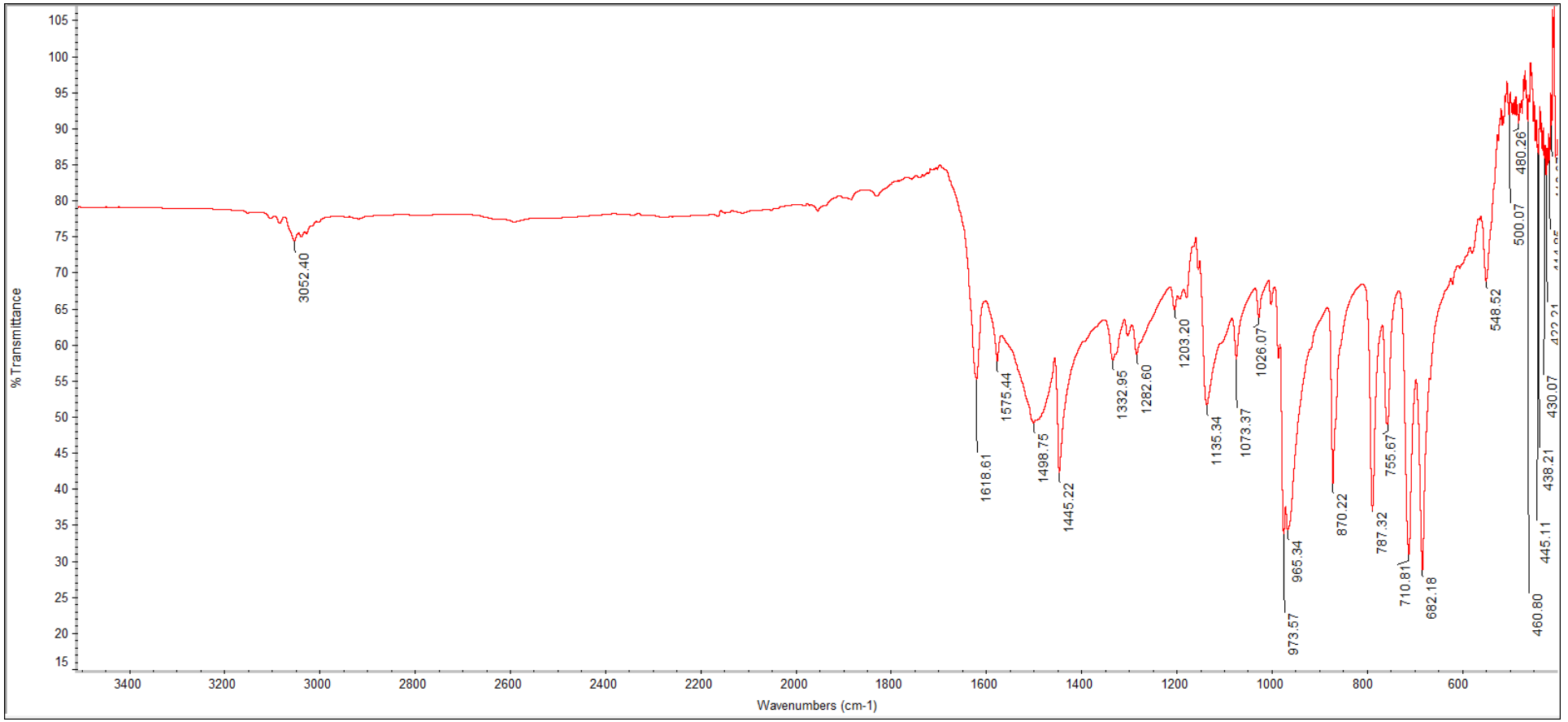

Figure S11: ATR-FTIR spectrum of **3**

Acquisition Parameter

Source Type	ESI	Ion Polarity	Negative	Set Nebulizer	0.3 Bar
Focus	Not active			Set Dry Heater	230 °C
Scan Begin	50 m/z	Set Capillary	2800 V	Set Dry Gas	3.0 l/min
Scan End	1000 m/z	Set End Plate Offset	-500 V	Set Divert Valve	Source

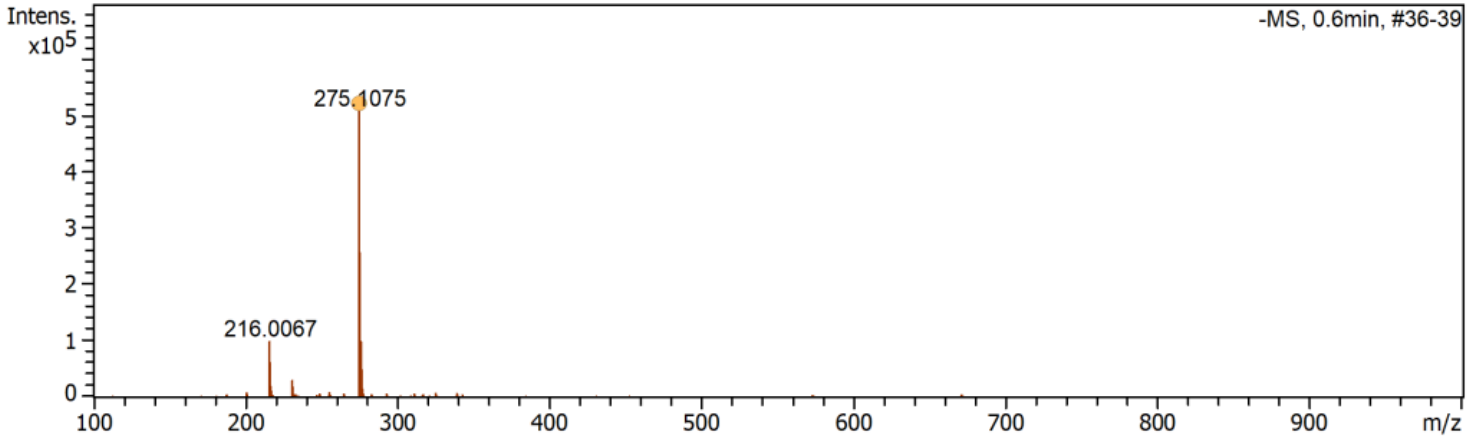

Meas. m/z	#	Ion Formula	m/z	err [ppm]	mSigma	#mSigma	Score	rdb	e¯ Conf	N-Rule
275.1075	1	C19H15O2	275.1078	0.8	8.3	1	100.00	12.0	even	ok

Figure S12: HRESIMS spectrum of **3**

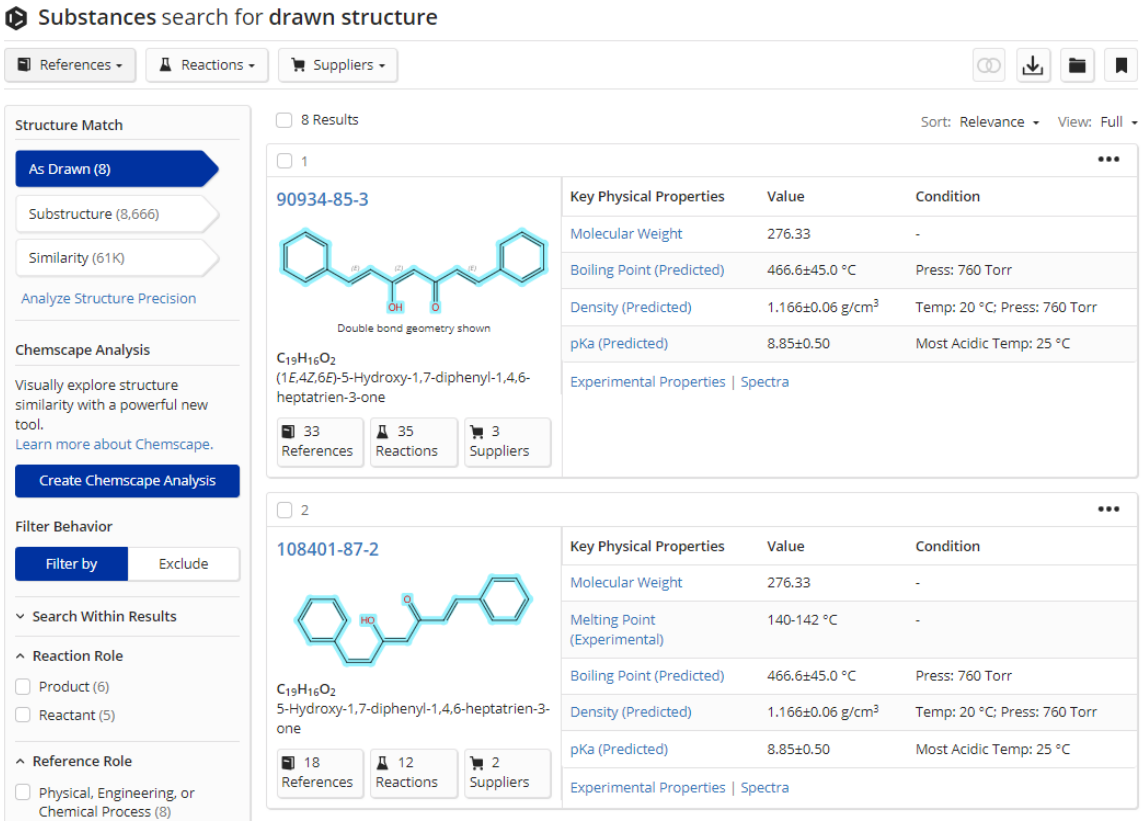

Figure S13: A SciFinder search report for **3** using the exact match option

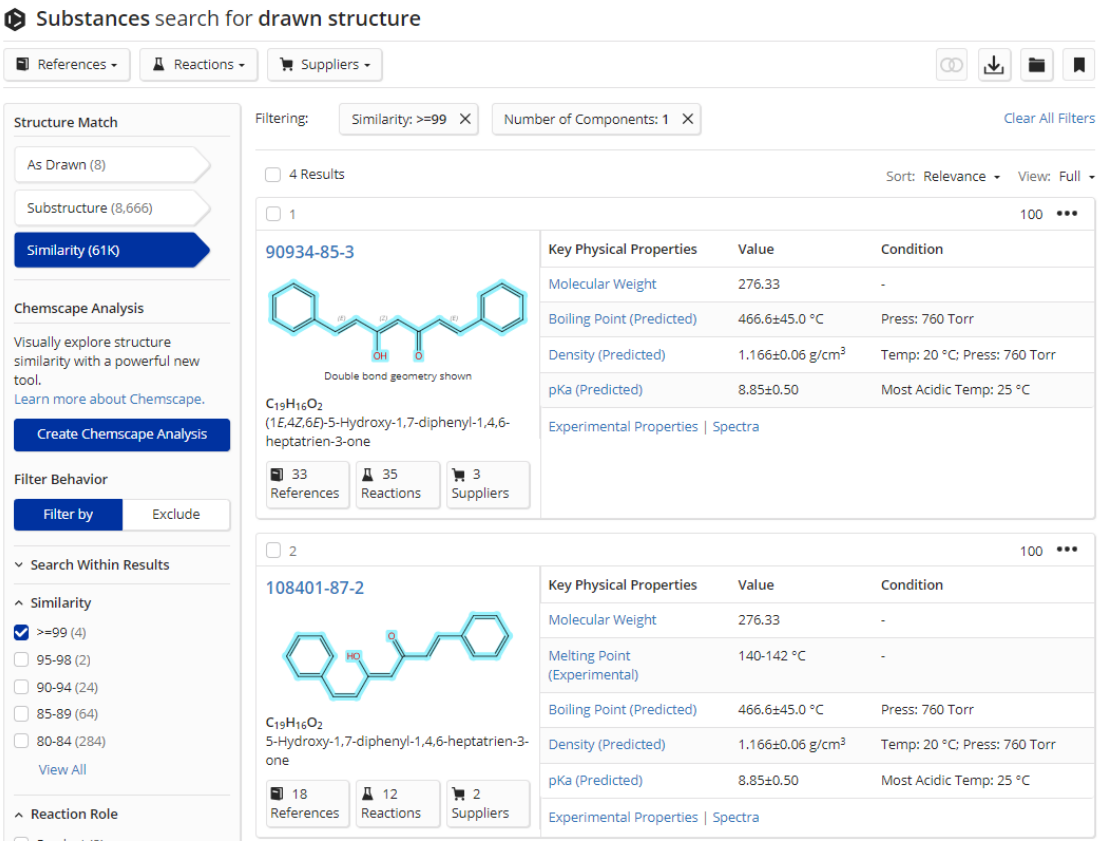

Figure S14: A SciFinder search report for **3** using the 99% similarity option

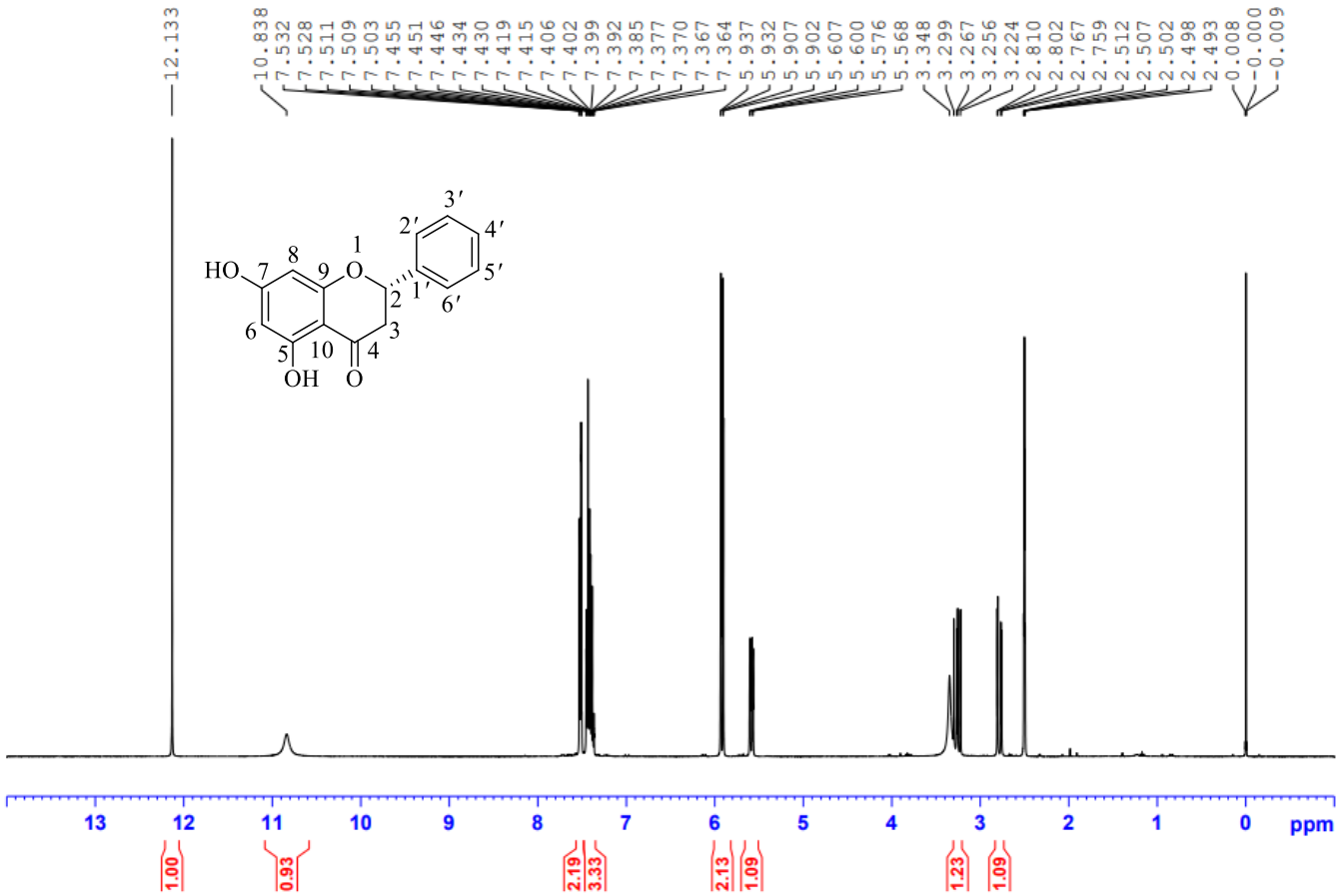

Figure S15: ^{1}H NMR spectrum of **4** (400 MHz, DMSO-d_6)

^{1}H NMR δ: 12.13 (*s*, 5-OH, 1H), 10.84 (*s*, 7-OH, 1H) 7.52 (*m*, H-2′, H-6′, 2H), 7.41 (*m*, H-3′, H-4′, H-5′, 3H), 5.93 (*d*, *J* = 2.0 Hz, H-6, 1H), 5.90 (*d*, *J* = 2.0 Hz, H-8, 1H), 5.68 (*dd*, *J* = 12.8, 3.2 Hz, H-2, 1H), 3.26 (*dd*, *J* = 17.2, 12.8 Hz, H-3β, 1H), 2.78 (*dd*, *J* = 17.2, 3.2, H-3α, 1H)

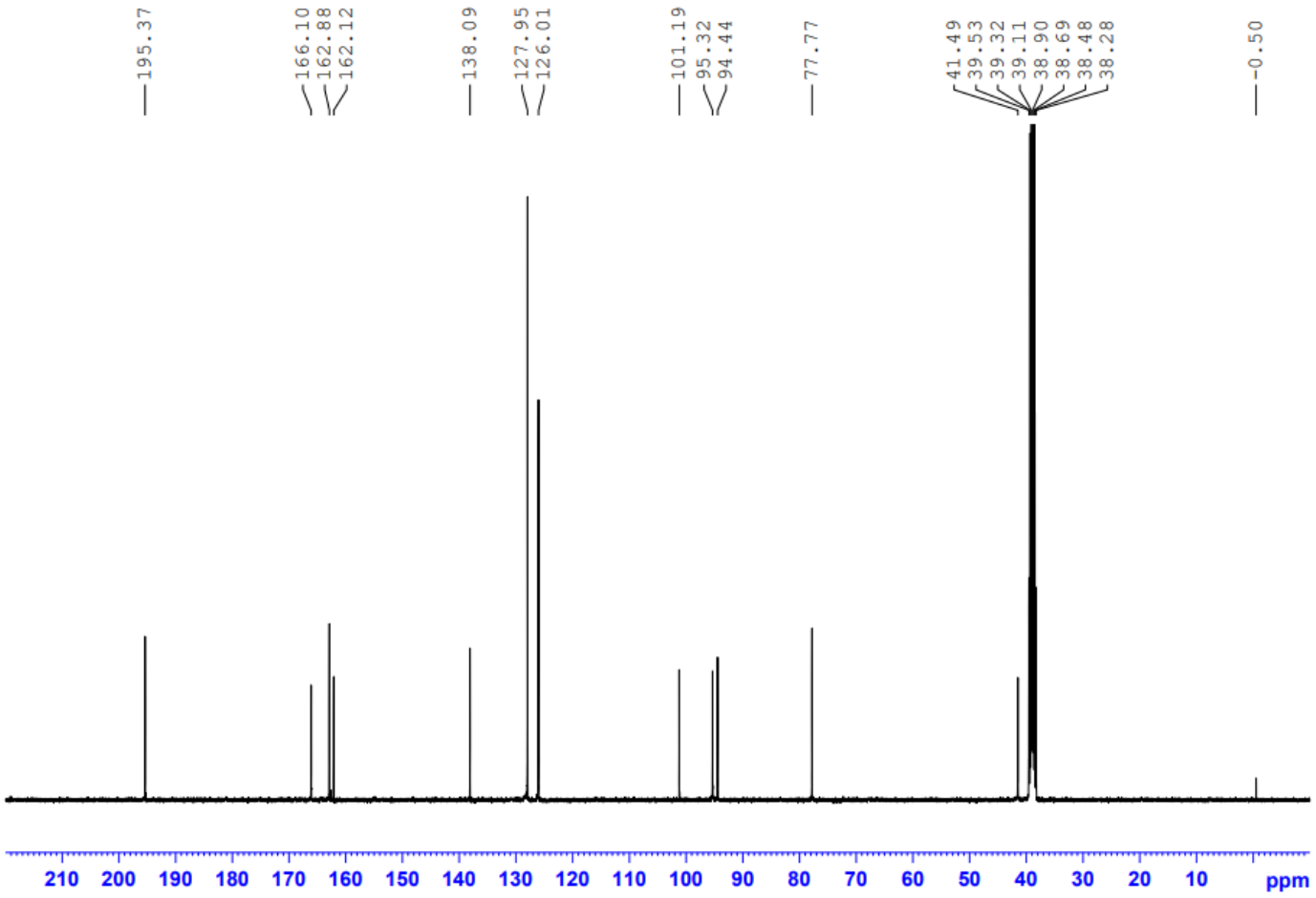

Figure S16: ^{13}C NMR spectrum of **4** (100 MHz, DMSO-d_6)

^{13}C NMR δ_C:195.4, 166.1, 162.9, 162.1, 138.1, 128.0 (2C), 126.0, 101.2, 95.3, 94.4, 77.7, 41.5. mp. 202–203 ^{o}C

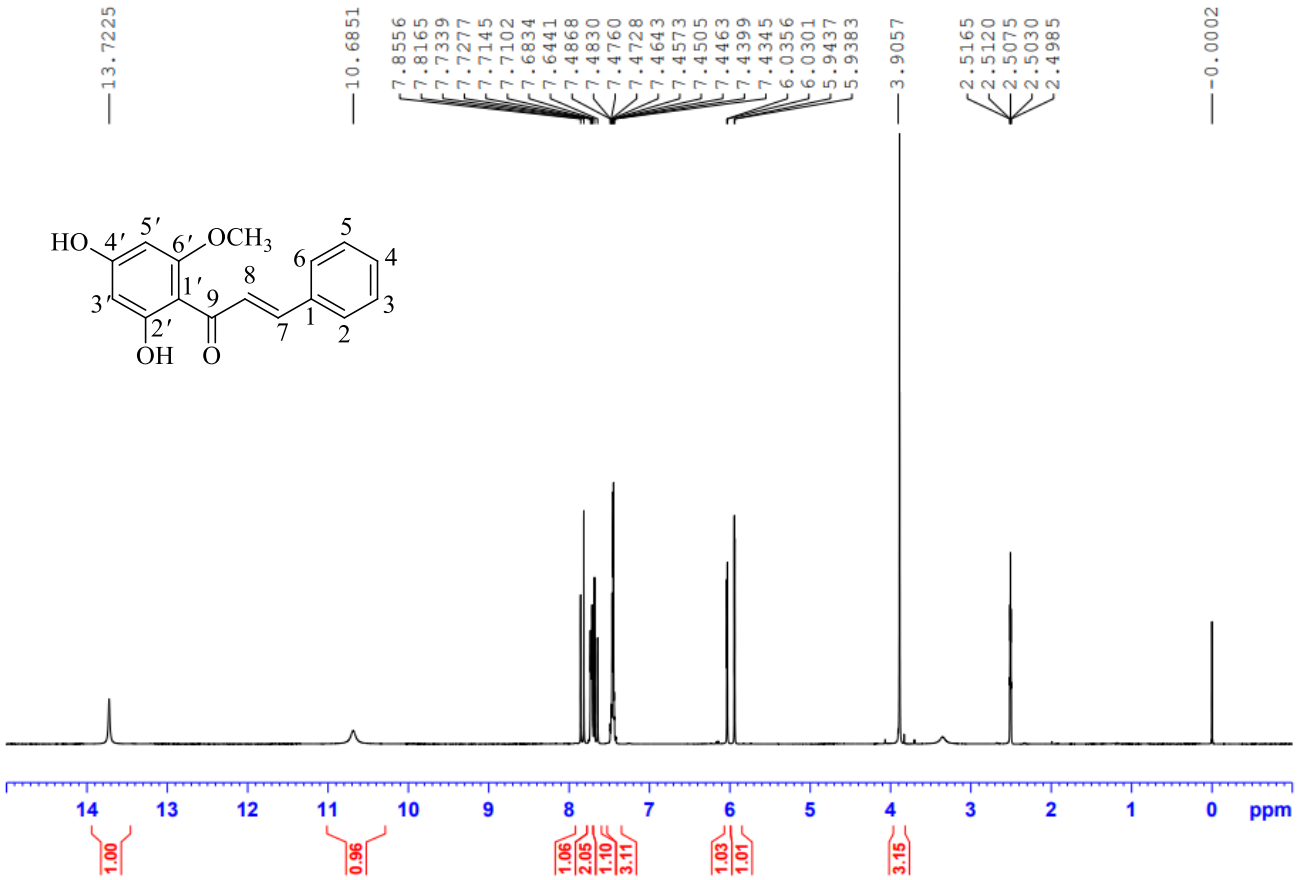

Figure S17: ^{1}H NMR spectrum of **5** (400 MHz, DMSO-d_6)

^{1}H NMR δ: 13.72 (*s*, 2′-OH, 1H), 10.69 (*s*, 4′-OH, 1H), 7.84 (*d*, *J* = 15.7 Hz, H-7, 1H), 7.72 (*m*, H-2, H-6, 2H), 7.66 (*d*, *J* = 15.7 Hz, H-8, 1H), 7.46 (*m*, H-3, H-4, H-5, 3H), 6.03 (*d*, *J* = 2.2 Hz, H-5′, 1H), 5.94 (*d*, *J* = 2.2 Hz, H-3′, 1H), 3.91 (*s*, 6′-OMe, 3H)

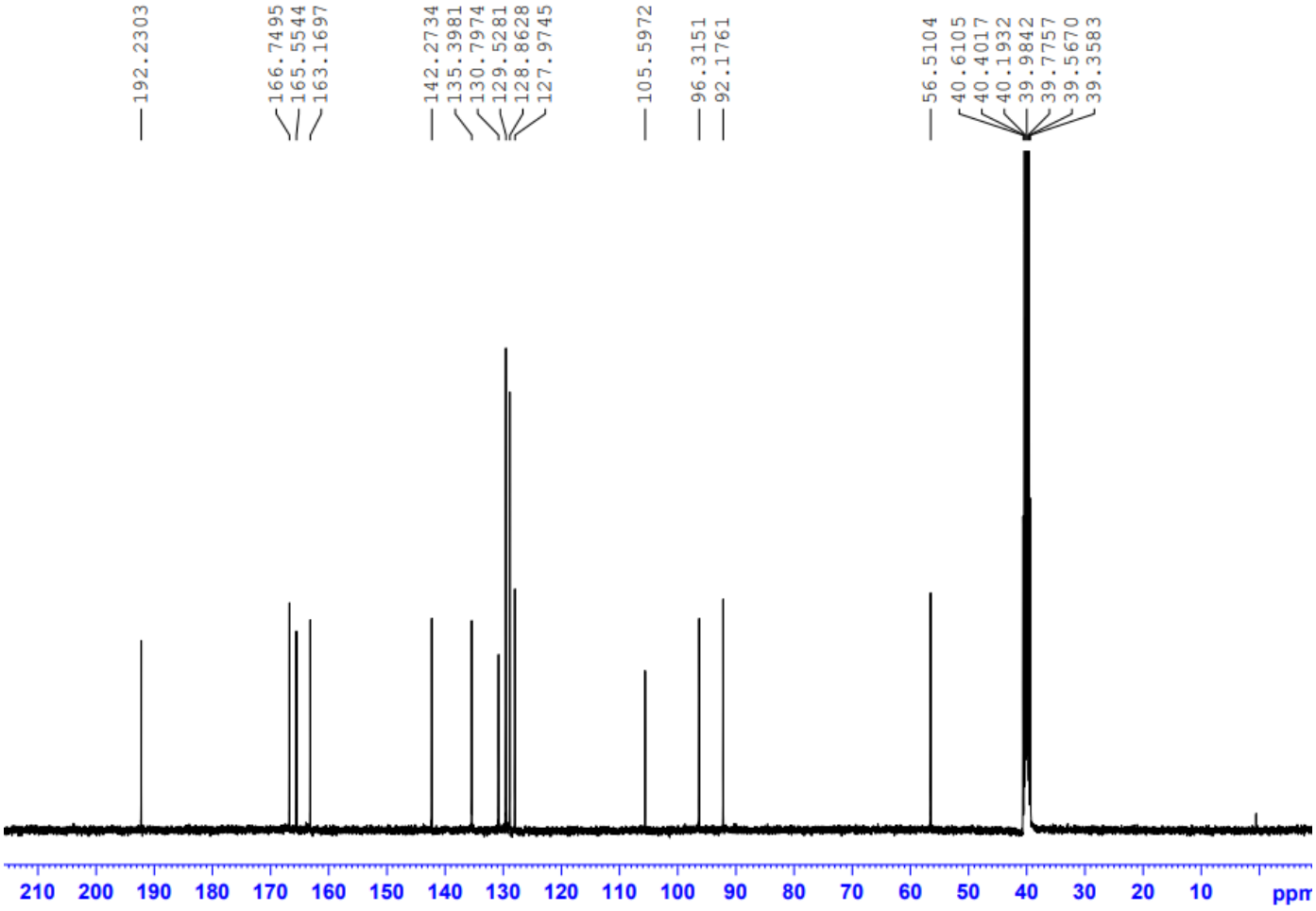

Figure S18: ^{13}C NMR spectrum of **5** (100 MHz, DMSO-d_6)

^{13}C NMR δ_C: 192.2, 166.8, 165.6, 163.2, 142.3, 135.4, 130.8, 129.5, 128.9, 128.0, 105.6, 96.3, 92.2, 56.5. mp. 200–201 ºC

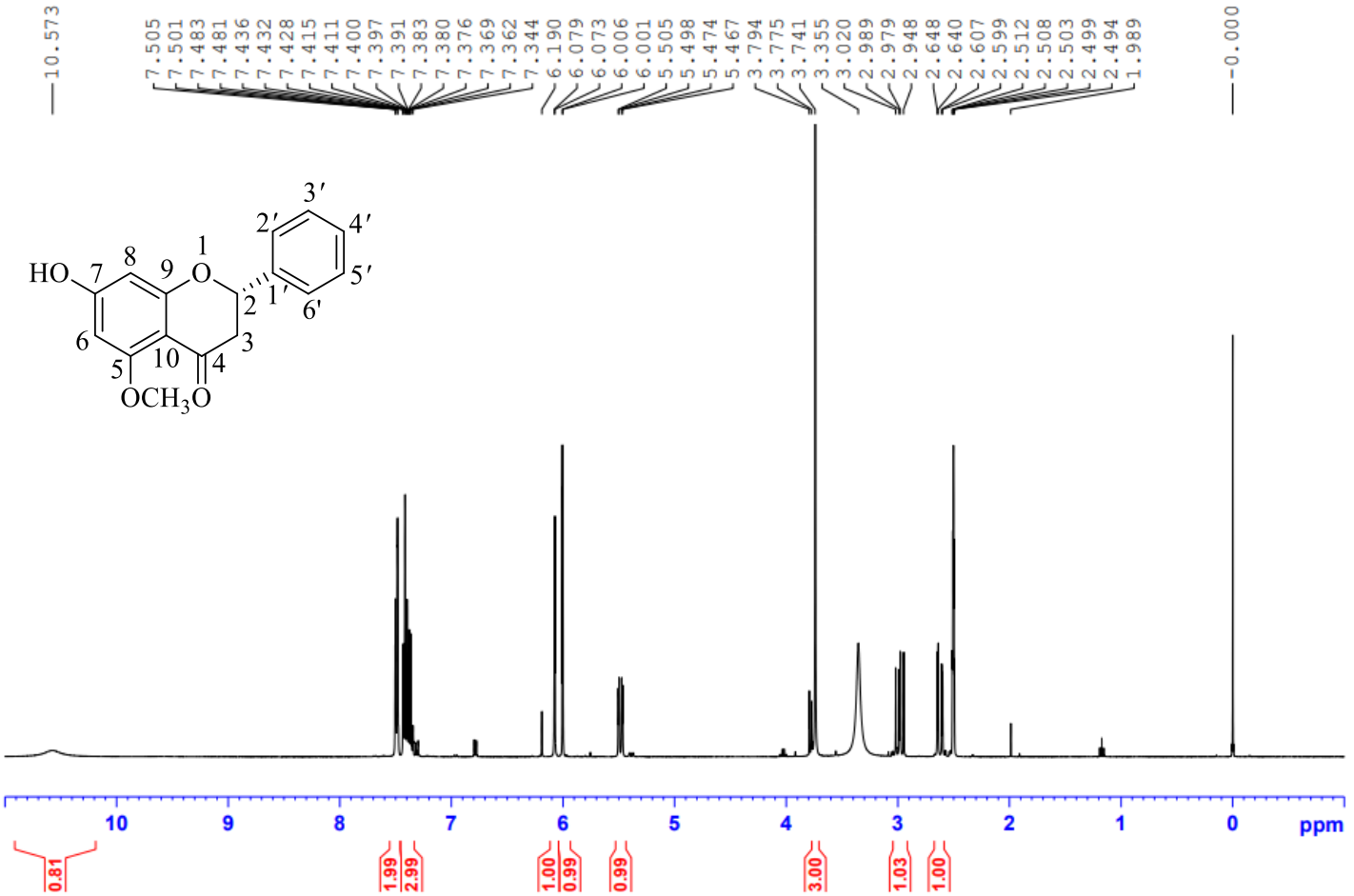

Figure S19: ^{1}H NMR spectrum of **6** (400 MHz, DMSO-d_6)

^{1}H NMR δ: 10.57 (*s*, 7-OH, 1H), 7.49 (*m*, H-2′, H-6′, 2H), 7.39 (*m*, H-3′, H-4′, H-5′, 3H), 6.08 (*d*, *J* = 2.4 Hz, H-8, 1H), 6.00 (*d*, *J* = 2.4 Hz, H-6, 1H), 5.84 (*dd*, *J* = 12.4, 3.2 Hz, H-2, 1H), 3.74 (*s*, C5-OMe, 3H), 2.98 (*dd*, *J* =16.4, 12.4 Hz, H-3β, 1H), 2.62 (*dd*, *J* = 16.4, 3.2 Hz, H-3α, 1H)

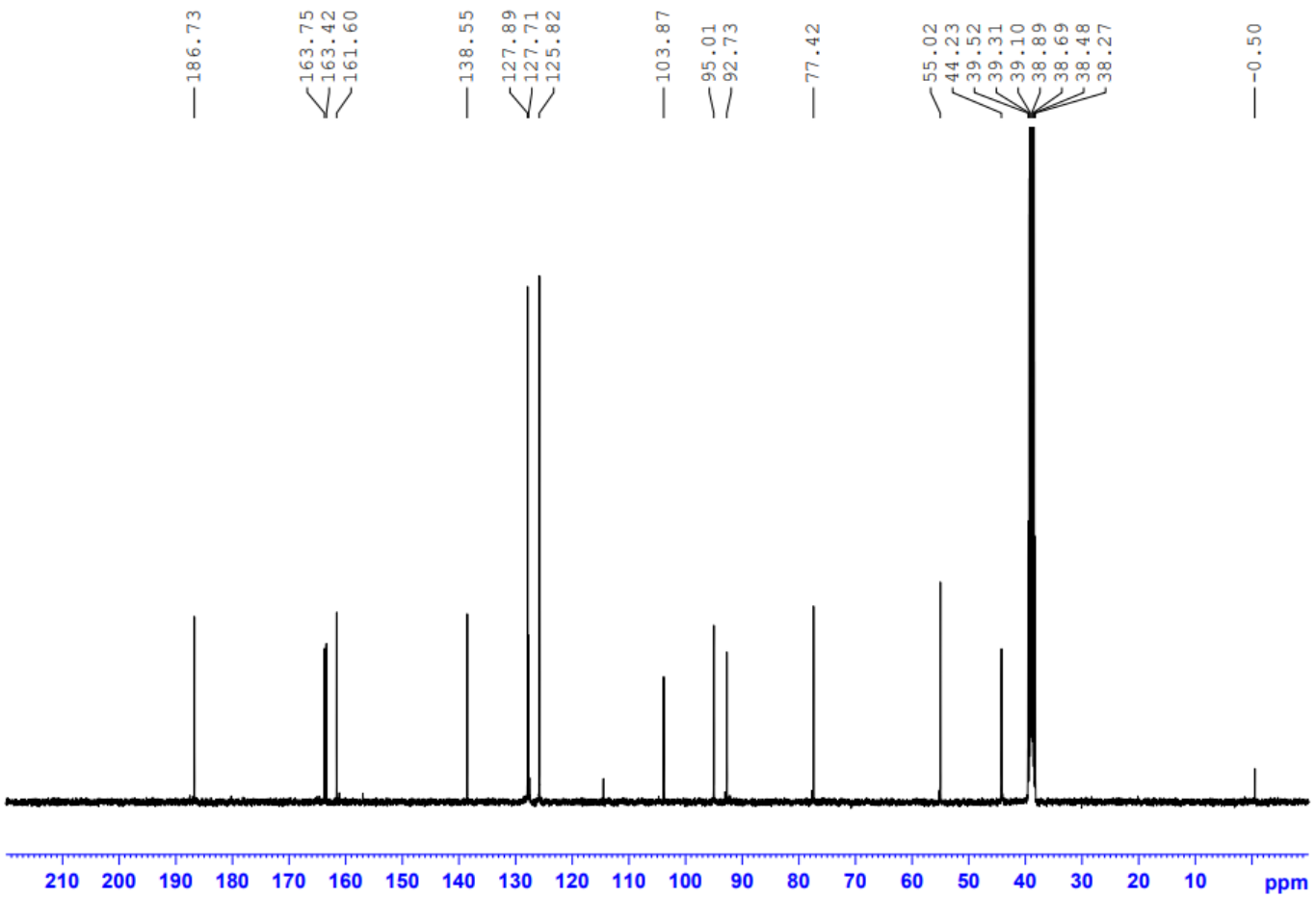

Figure S20: ^{13}C NMR spectrum of **6** (100 MHz, DMSO-d_6)

^{13}C NMR δ_C: 186.7, 163.8, 163.4, 161.6, 138.6, 127.9, 127.7, 125.8, 103.9, 95.0, 92.7, 77.4, 55.0, 44.2. mp. 222–223.5 ^{o}C

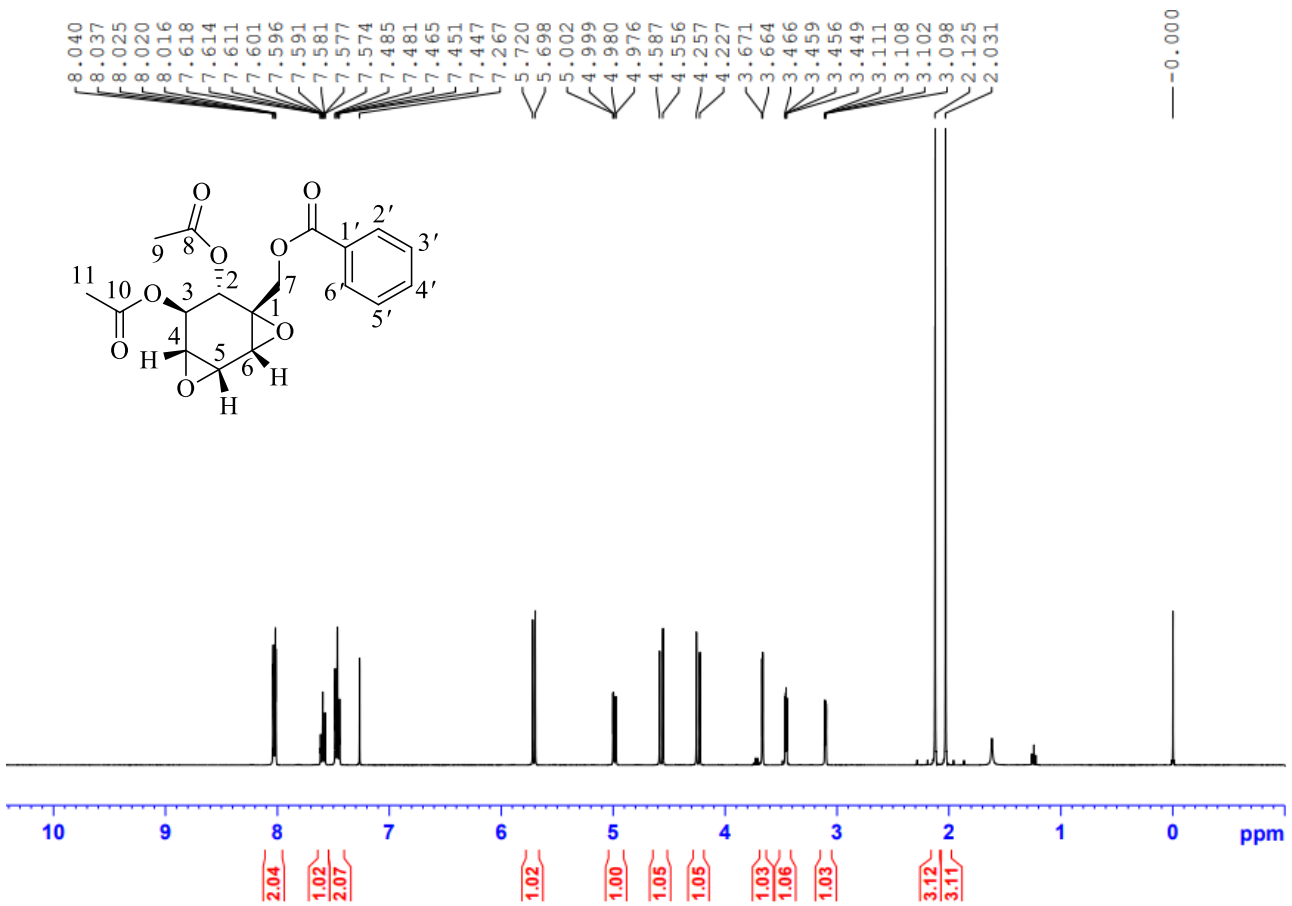

Figure S21: ^{1}H NMR spectrum of **7** (400 MHz, $CDCl_3$)

^{1}H NMR δ: 8.03 (*m*, H-2′, H-6′, 2H), 7.60 (*tt*, *J* = 8.0, 1.6 Hz, H-4′, 1H), 7.46 (overlapping signal, H-3′, H-5′, 2H), 5.71 (*d*, *J* = 8.8 Hz, H-2, 1H), 4.99 (*dd*, *J* = 8.8, 1.2 Hz, H-3, 1H), 4.57 (*d*, *J* = 12.4 Hz, H-7a, 1H), 4.24 (*d*, *J* = 12.4 Hz, H-7b, 1H), 3.67 (*d*, *J* = 2.8 Hz, H-6, 1H), 3.46 (*dd*, *J* = 4.0, 2.8 Hz, H-5, 1H) 3.10 (*dd*, *J* = 4.0, 1.2 Hz, H-4, 1H), 2.12 (*s*, H-11, 3H), 2.03 (*s*, H-9, 3H)

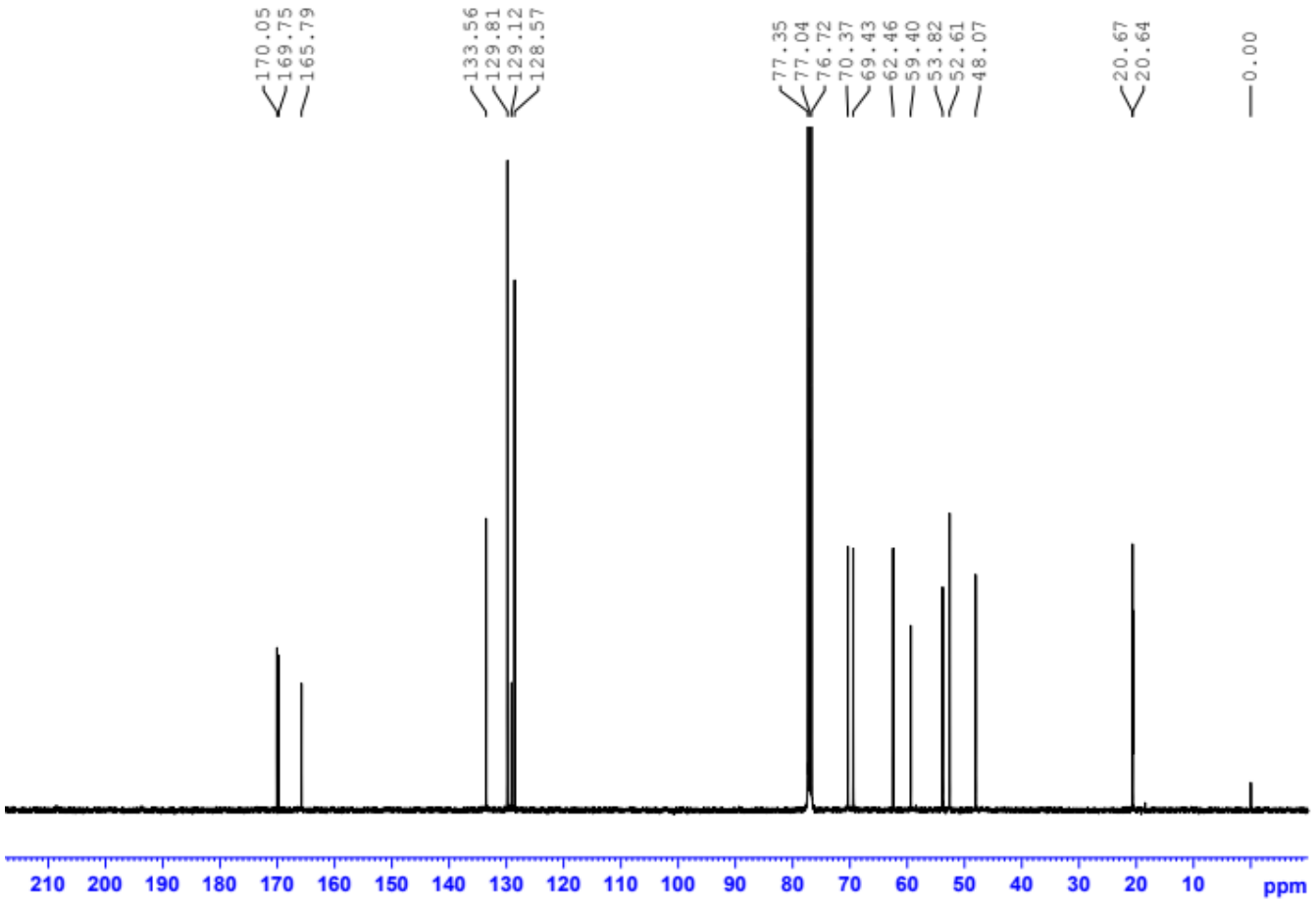

Figure S22: ^{13}C NMR spectrum of **7** (100 MHz, $CDCl_3$)

^{13}C NMR δ_C: 170.1, 169.8, 165.8, 133.6, 129.8 (2C), 129.1, 128.6 (2C), 70.4, 69.4, 62.5, 59.4, 53.8, 52.6, 48.1, 20.7, 20.6. mp. 152.4–152.8 °C. $[\alpha]_D^{28}$ + 38.4318 (*c* 0.44, CH_2Cl_2)

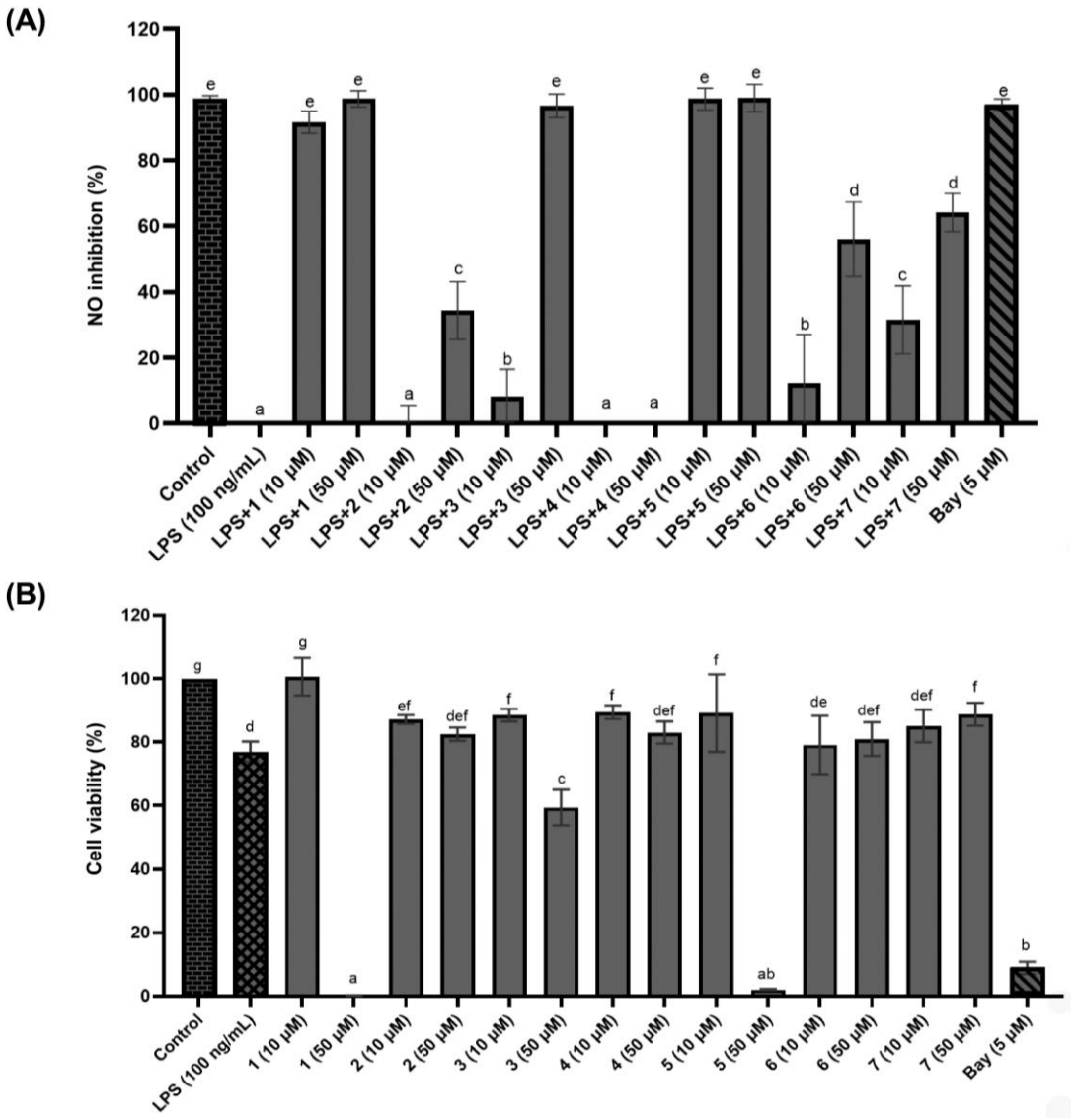

Figure S23: Effect of pretreatment with compounds **1–7** isolated from *K. elegans* on inflammation and cellular cytotoxicity in lipopolysaccharide (LPS)-stimulated macrophage cells. **A)** Percentage of nitric oxide (NO) inhibition, **B)** percentage of cell viability. One-way ANOVA was performed to determine the mean values, with significant differences at *p* value of <0.05 indicated by different letters

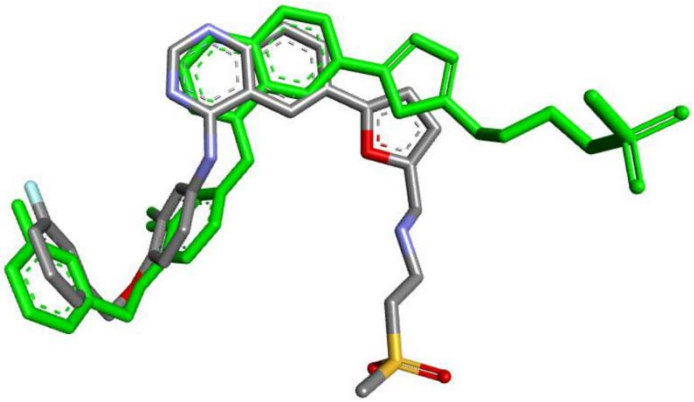

Figure S24: Superimposition of the lowest energy conformer of docked lapatinib and the co-crystallised lapatinib in the EGFR binding site. The calculated RMSD value for heavy atoms equates to 3.58 Å. The calculated GoldScore value is 97.46 for the lowest energy docked conformer

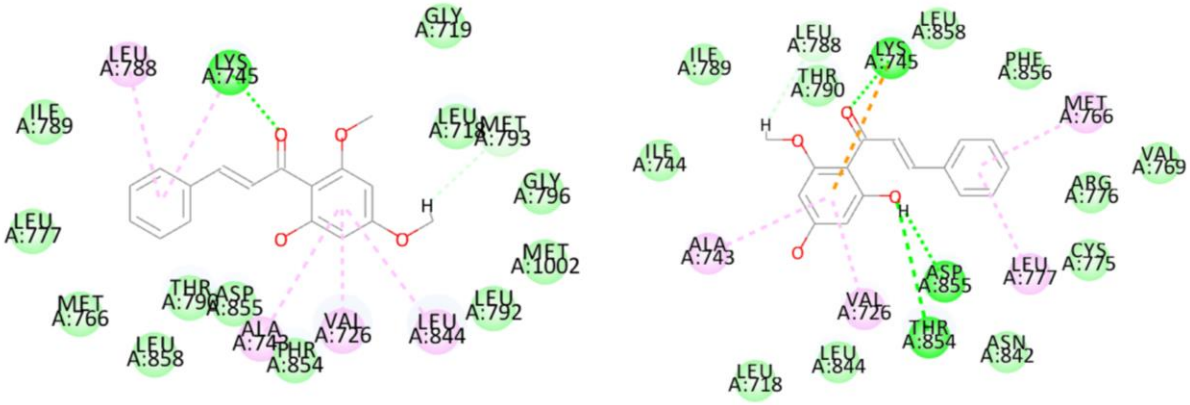

Figure S25: The binding interactions represented in 2D format between EGFR protein and the molecules, flavokawain B (**1**) and cardamonin (**5**). Green dotted lines represent hydrogen bonds, orange and pink dotted lines represent dipole-dipole interactions. Residues with light green shades depict residues that are able to form hydrophobic interactions

S1: Experimental

Chemicals and Instrumentation

Melting points were measured using a Buchi B-540 apparatus (Buchi, Switzerland). Infrared (IR) spectroscopy and mass spectrometry (MS) measurements were performed using a Perkin Elmer Spectrum ONE (Perkin Elmer, USA) and a Compact Mass Spectrometry (CMS) (Advion, USA), respectively. ^{1}H and ^{13}C NMR spectra were recorded on Bruker Avance III HD 400 spectrometers operating at 400 and 100 MHz, respectively. Optical rotations were measured on a P-1020 polarimeter (JASCO, Japan). Silica gel column chromatography was performed using Kieselgel 60 (70–230 mesh) (Merck, Germany). Kieselgel 60, F_{254} (230–400 mesh) (Merck, Germany) was used for TLC. To detect the compounds, they were first visualized under UV light and then sprayed with phosphomolybdic acid reagent, followed by heating at 80℃ for 2–3 min.

Cell Culture

Cells were cultured in complete Dulbecco's modified Eagle medium (DMEM, Hyclone) supplemented with 1% of antibiotics (penicillin/streptomycin), 1% 4-[2-hydroxyethyl]-1-piperazine ethanesulfonic acid (HEPES, Hyclone), 1% sodium pyruvate (Hyclone), and 10% of fetal bovine serum (FBS, Hyclone) and maintained in a humidified incubator at 37℃ with 5% CO_2.

Cytotoxicity Evaluation

The cytotoxicity of pure compounds against human breast cancer (MCF-7 and MDA-MB-231 cells) and human liver cancer (Huh-7 and SNU449 cells) was tested using the colorimetric method via the MTT assay [1]. Cell lines at a density of 5×10^3 cells/well were seeded in a 96-well plate for 24 hours. Various concentrations of test compounds were added to the 96-well plate and incubated for 48 hours. Ten microliters of MTT solution (5 mg/mL) were added and incubated for 2 hours. Then, cell supernatants were removed, and dimethylsulfoxide (DMSO) was added to dissolve the formazan product. The light absorbance was measured at 570 nm using a microplate spectrophotometer. The IC_{50} value was calculated using GraphPad Prism version 8.

Cell Viability Assay for RAW264.7 Macrophage Cells

An MTT assay was performed to determine the macrophage cell viability [2]. In brief, RAW264.7 cells were seeded in 96-well plates at a density of 10,000 cells/well overnight. Then, the cells were incubated with complete media containing vehicle control, lipopolysaccharide (LPS; 100 ng/mL), or test compounds at final concentrations of 10 and 50 µM. After incubation for 24 hours, the culture medium was removed, and the cells were subsequently incubated with the MTT solution (5 mg/mL) at 37℃ for 3 hours. The medium was removed, and the reaction was solubilized with DMSO (100 µL). The absorbance was measured at 570 nm using a microplate reader.

Nitric Oxide (NO) Inflammation Assay

The nitrite accumulation in culture supernatant was determined to measure the production of nitrite using a colorimetric reaction [2]. RAW264.7 cells were seeded onto 96-well plates at a density of 10,000 cells/well overnight. The cells were pretreated with vehicle control or test compounds (10 and 50 µM) or Bay11 (5 µM) as a positive control, which was diluted in 100 µL/well of complete media. After preincubation for 1 hour, the cells were stimulated with 100 ng/mL of LPS for a further 24 hours. Culture supernatants (50 µL) were collected and transferred to u-bottom 96 well plates.

Next, 50 µL of Griess reagent was added to each well and incubated at room temperature for 15 minutes. The absorbance at 540 nm was determined using a PerkinElmer Ensight Multimode Microplate Reader. The absorbance values were compared with a standard sodium nitrite curve. The percentage of NO inhibition was determined as follows:

$$\%\ NO\ inhibition = 100 - \left[\frac{Nitrite\ concentration\ of\ sample}{Nitrite\ concentration\ of\ LPS}\ x\ 100\right]$$

Molecular Modeling

The ligands were constructed using Chem3D Pro 12.0 and the chemical structures were drawn and energy-minimized using the MM2 [3] force field and saved in 3D format. The crystal structure of EGFR was obtained from the Protein Data Bank (PDB) [4] ID:1XKK [5] with a resolution of 2.40 Å. Discovery studio version 4.5 was used to prepare the crystal structure for docking, i.e., hydrogen atoms were added and the crystallographic solvents and cocrystallized ligand were removed. The center of the EGFR binding site was defined at coordinates of x = 12.683, y = 33.305, and z = 37.276 with a radius of 10 Å. The basic amino acids lysine and arginine were defined as protonated, whereas aspartic and glutamic acids were assumed to be deprotonated. The GoldScore (GS) [6] scoring function was implemented for docking the ligands using the Genetic Optimisation for Ligand Docking software package (GOLD) version 2023.1.0. Molecular docking was conducted at 100% efficiency at 50 docking runs per ligand.

References

[1] C. Thepmalee, N. Sawasdee, P. Jenkham, C. Thephinlap, K. Khoothiam, N. Suwannasom, R. Chokchaisiri, A. Panya and P.T. Yenchitsomanus (2023). Anti-cancer effect of a phytochemical compound - 7R-acetylmelodorinol - against triple-negative breast cancer cells, *Biomed. Pharmacother.* **166**, 115286-115297.

[2] E.R. Sukandar, S. Kaennakam, S. Wongsuwan, J. Chatwichien, S. Krobthong, Y. Yingchutrakul, T. Mahatnirunkul, F. Mulya, V. Parasuk, D.J. Harding, P. Poldorn, T. Rungrotmongkol, S. Tip-pyang, C. Aonbangkhen and W. Chavasiri (2023). Schomburginones A–J, geranylated benzophenones from the leaves of *Garcinia schomburgkiana* and their cytotoxic and anti-inflammatory activities, *Phytochem.* **211**, 113701.

[3] N.L. Allinger (1977). Conformational analysis. 130. MM2. A hydrocarbon force field utilizing V1 and V2 torsional terms, *J. Am. Chem. Soc.* **99(25)**, 8127-8134.

[4] H.M. Berman, J. Westbrook, Z. Feng, G. Gilliland, T.N. Bhat, H. Weissig, I.N. Shindyalov and P.E. Bourne (2000). The Protein Data Bank, *Nucleic Acids Res.* **28(1)**, 235-242.

[5] E.R. Wood, A.T. Truesdale, O.B. McDonald, D. Yuan, A. Hassell, S.H. Dickerson, B. Ellis, C. Pennisi, E. Horne, K. Lackey, K.J. Alligood, D.W. Rusnak, T.M. Gilmer and L. Shewchuk (2004). A unique structure for epidermal growth factor receptor bound to GW572016 (Lapatinib): relationships among protein conformation, inhibitor off-rate, and receptor activity in tumor cells, *Cancer Res.* **64(18)**, 6652-6659.

[6] M.L. Verdonk, J.C. Cole, M.J. Hartshorn, C.W. Murray and R.D. Taylor (2003). Improved protein-ligand docking using GOLD, *Proteins* **52(4)**, 609-623.